CHARACTERISTICS OF APOLLO-TYPE LUNAR ORBITS

by
George H. Born

TCR 7 June 6, 1966

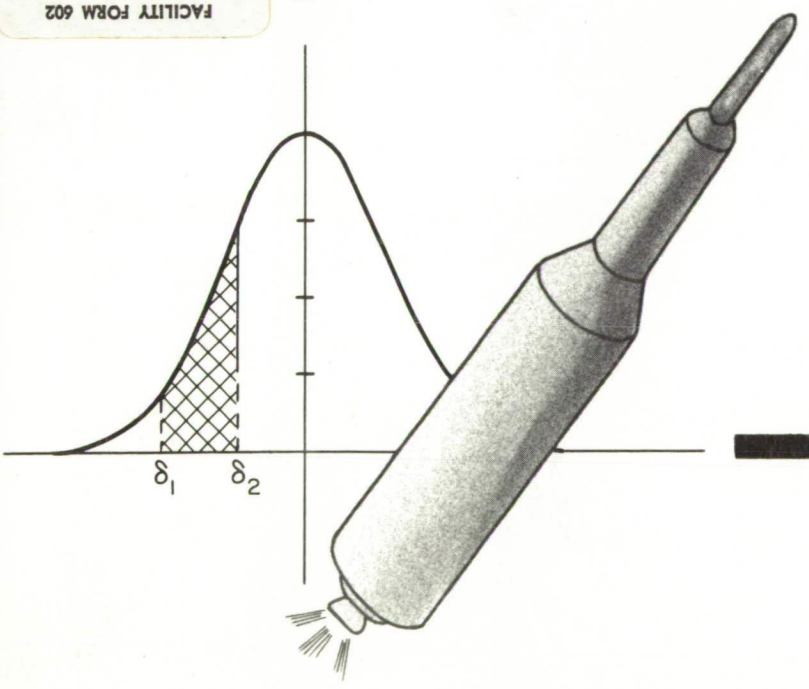

TEXAS CENTER FOR RESEARCH
P. O. BOX 8472, UNIVERSITY STATION, AUSTIN, TEXAS

This report was prepared under

NASA MANNED SPACE FLIGHT CENTER
Contract 9-2619

under the direction of

Dr. Byron D. Tapley

Associate Professor of Aerospace Engineering

and Engineering Mechanics

CHARACTERISTICS OF APOLLO-TYPE LUNAR ORBITS

by

GEORGE H. BORN, B.S.

THESIS

Presented to the Faculty of the Graduate School of

The University of Texas in Partial Fulfillment

of the Requirements

For the Degree of

MASTER OF SCIENCE IN AERO-SPACE ENGINEERING

THE UNIVERSITY OF TEXAS

JANUARY, 1965

A B S T R A C T

A computer routine for numerically integrating Lagrange's Planetary Equations for lunar satellite orbits was revised to integrate an alternate set of perturbation equations which do not have the small eccentricity restriction of Lagrange's Equations. This set of equations was solved numerically for the time variations of the orbit elements of circular lunar satellite orbits. Consideration was given to orbits with near equatorial inclinations and low altitudes similar to those considered for the Apollo Project.

The principal perturbing forces acting on the satellite were assumed to be the triaxiality of the Moon and the mass of the Earth. The Earth was considered as a point mass revolving in an elliptical orbit about the Moon.

The variations with time of the orbit elements for twelve sets of initial conditions were investigated. Data showing the results for both short time, three revolutions of the satellite, and long time, 80 revolutions of the satellite, are presented in both tabular and graphical form.

TABLE OF CONTENTS

L I S T O F F I G U R E S

FIGURE PAGE

L I S T O F T A B L E S

N O M E N C L A T U R E

A_1	Principle moment of inertia about x' axis
A'	$L_m - L_s$
A	e cos ω
[A]	Coordinate transformation matrix
a	Semi-major axis of the satellite orbit
B_1	Principle moment of inertia about y' axis
B'	$L_m - \tilde{\omega}_m$
B	e sin ω
C_1	Principle moment of inertia about z' axis
C'	$L_s - \tilde{\omega}_s$
C	Perturbative acceleration in circumferential direction
D'	$L_m - \Omega_m$
D	Elongation of Moon
E	Eccentric anomaly of satellite orbit
e	Eccentricity of satellite orbit
$\overline{F}$	Perturbing force
f	True anomaly
G	Universal gravitational constant
H	Perturbing force potential
h	Angular momentum
I	Inclination of satellite orbit plane to lunar equator
I_e	Inclination of Earth-Moon orbit plane to lunar equator

$\bar{i},\bar{j},\bar{k}$	Unit vectors in (x,y,z) direction
$\bar{i}_n$	Unit vector in direction of ascending node of Moon's orbit about the Earth
$\bar{i}_\xi$	Unit vector in direction of lunar perigee
L_m	Geocentric mean longitude of Moon
L_s	Geocentric mean longitude of Sun
M	Mass of the satellite
M_e	Mass of the Earth
M_m	Mass of the Moon
P	Semi-latus rectum
R	Perturbative force in radial direction
r_e	Radius of Earth
r_{es}	Radius from Earth to satellite
t	Time
t_p	Time of previous pericenter passage
u	Angle measured from ascending node to satellite radius vector
V	Velocity
V_t	Total potential energy function
V_m	Potential energy function of Moon
V_e	Potential energy function of Earth
W	Perturbative acceleration normal to orbital plane
x,y,z	Selenocentric inertial coordinates
x',y',z'	Selenocentric rotating coordinates
x_e,y_e,z_e	Coordinates of Earth

$\ddot{X},\ddot{Y},\ddot{Z}$	Perturbative accelerations in x,y,z direction
$\bar{\ddot{X}},\bar{\ddot{Y}},\bar{\ddot{Z}}$	Total acceleration in x,y,z direction
β	Latitude
$\bar{\epsilon}_{(\ )}$	Unit vector in the subscript direction
λ	Longitude
θ	Angle between line of nodes and x' axis
θ_e	Angle between line of nodes and radius vector of Earth
θ_o	Phase angle between x axis and periselene
μ_m	Lunar gravitational potential
ω	Argument of pericenter
ω_e	Angular velocity of Earth with respect to Moon
$\tilde{\omega}_m$	Geocentric mean longitude of Moon's perigee
$\tilde{\omega}_s$	Geocentric mean longitude of Sun's perigee
Ω_m	Geocentric mean longitude of Moon's ascending node
Ω	Longitude of ascending node of satellite
$\bar{(\ )}$	Vector notation
$\dot{(\ )}$	First derivative of ( ) with respect to time
$\ddot{(\ )}$	Second derivative of ( ) with respect to time

C O N S T A N T S

a	384422 KM
A_1	$.887825 \times 10^{29}$ KG KM^2
B_1	$.888005 \times 10^{29}$ KG KM^2
C_1	$.888375 \times 10^{29}$ KG KM^2
e	.0549
G	$.66709998 \times 10^{-19}$ $KM^3/KG/sec^2$
I_e	.116384501 radians
M_e	$.597516432 \times 10^{25}$ KG
M_m	$.73464634 \times 10^{23}$ KG
r_m	$.173999208 \times 10^{4}$ KM
μ_e	$.39860320 \times 10^{6}$ KM^3/sec^2
μ_m	$.49027779 \times 10^{4}$ KM^3/sec^2
ω_e	$.266507564 \times 10^{-5}$ radians/sec

I. INTRODUCTION

With the recommendation of the President and the approval of Congress, the United States of America has launched the scientific and technicological undertaking of manned exploration of the Moon. The program has been assigned to the National Aeronautics and Space Administration and has been titled "Project Apollo."

One prerequisite to lunar landing is the establishment of the Apollo spacecraft in a lunar orbit. It is necessary that the variation of this orbit with time be known in order:

(1) To effect a landing in a preselected area of the lunar surface, and

(2) To establish stay times on the lunar surface in order to assure successful completion of rendezvous with the command module during the return to lunar orbit.

The necessity of determing the characteristics of Apollo-type lunar orbits prompted the investigation described here.

The investigation of Earth satellite motion has been quite thorough, however, a relatively small amount of

work has been done in lunar satellite theory because significant interest in this area has developed comparatively recently. There are several reasons why the theory of terrestrial satellite motion is not directly applicable to lunar satellites. While usually the mass of the Moon is neglected in studies of Earth satellite motion, the greater mass of the Earth has a significant influence on the motion of a lunar satellite. Also, one of the first assumptions in most investigations of Earth satellite motion is that the Earth is a spheroid of revolution. The Moon, however, is best approximated as a triaxial ellipsoid; i.e. the Moon is not a body of revolution. Therefore, it has no plane of symmetry. Consequently, the lunar gravitational field is more complex than the gravitational field of the Earth. Moreover, its orientation with respect to an inertial coordinate system is changing with time due to the rotation of the Moon about its axis. Due to these factors, the problem of describing the motion of a near lunar satellite is in general a different and more complex problem than that of describing the motion of a near Earth satellite. It should be noted that the presence of atmospheric drag, which greatly complicates the motion of near Earth satellites, is of no consequence in the motion of lunar satellites.

A survey of the literature concerned with this problem reveals that the primary effort, thus far, has been the development of approximate closed form solutions to Lagrange's Planetary Equations, which are a set of first order, nonlinear, differential equations for the time rates of change of the orbit elements. Lass and Solloway (Reference 10)* have developed approximate solutions to these equations for near circular orbits using the averaging process of Kryloff-Bogolinboff. For this analysis the Moon was assumed to be a triaxial ellipsoid in a circular orbit about a point mass Earth. The effects of the Sun were neglected after they were shown to be on the order of 0.005 times the effects of the Earth. Lorell (Reference 11) presents some of the long term and secular effects of the Earth, Sun, and lunar gravitational potential on lunar satellite orbits for the same Earth-Moon model. Tolson (Reference 15) has developed a first order approximation to the motion of a lunar satellite under the influence of only the Moon's noncentral force field.

A few published results exist which deal with numerically integrating the perturbation equations. Two

---

*References appear on pp. 71-72.

such efforts by Brumberg and Goddard are recorded in References 3 and 5 respectively. Brumberg considers the Earth and Sun to be point masses and the Moon a triaxial ellipsoid. Goddard neglects the effects of the Sun and considers the Earth as a point mass in a circular orbit about the Moon. Each of the authors considers polar and equatorial orbits of both large and small eccentricity. The integrations are carried out over a period of 40 revolutions, and both authors conclude that these orbits exhibit a high degree of stability. However, these investigations deal with orbits of greater altitude and eccentricity than the Apollo-type orbits.

The analysis presented here is concerned with the derivation and numerical integration of a set of differential equations for the time rate of change of the orbit elements for circular lunar satellite orbits of low altitude, 50 to 150 miles, and near equatorial inclinations of 0.5° to 20° (direct orbits) and 160° to 179.5° (retrograde orbits). Integrations were carried out over a period of 80 revolutions of the satellite. This corresponds to a time interval of 7 to 8 Earth days. The results, indicating the variation with time of the orbit elements, are presented in numerical and graphical form.

II. ANALYSIS

A. Motion of the Earth-Moon System

Before formulating the problem, the motion of the Earth-Moon system will be reviewed.

The Earth-Moon system revolves about its center of mass, the barycenter, with a period of 27.32 Earth days. Because of the larger mass of the Earth ($\frac{Me}{Mm} = 81.32$), the barycenter lies within the radius of the Earth. The effects of the Sun and planets as well as the asphericity of the Earth and Moon result in the Earth-Moon orbit being a perturbed ellipse with an average orbital eccentricity of 0.0549. The average distance between mass centers of the Earth and the Moon is 384,000 km (238,600 miles).

As seen from above the Northern hemisphere, the directions of the Earth's rotation about the Sun and the Moon's rotation about the Earth are westward or counterclockwise.

The line of intersection of the Moon's orbit plane with the ecliptic (plane of Earth's orbit about the Sun) is called the line of nodes. Due primarily to the perturbing influence of the Earth and the Sun, the line of nodes regresses westward with a period of 18.6 Earth years, and the line of apsides, or major axis of the lunar orbit, rotates eastward with a period of 8.85 Earth years.

The inclination of the Moon's equatorial plane to the ecliptic is practically fixed at 1°32', while the inclination of the plane of the Earth-Moon orbit to the ecliptic is 5°9' (Figure 1). This accounts for the fact that an observer on Earth would at one time see the north pole of the Moon (position A in Figure 1) and half a month later see the south pole (position B in Figure 1). This apparent oscillation in the Moon's poles is called the "optical libration in latitude." Since the Moon moves in an elliptical orbit and its spin rate is practically constant, to an observer on Earth the Moon would appear to oscillate about its spin axis. This apparent oscillation is called the "optical libration in longitude." These librations in latitude and longitude result in the eventual exposure of 59 per cent of the lunar surface to an Earth observer.

B. Problem Definition and Assumptions

Since the Moon is not spherical and since bodies of the Solar System exert a mutual influence on each other, the motion of a lunar satellite is not a simple ellipse such as that associated with ideal two-body motion. Its motion can, however, be described in terms of the so-called osculating ellipse. The osculating ellipse is an ellipse

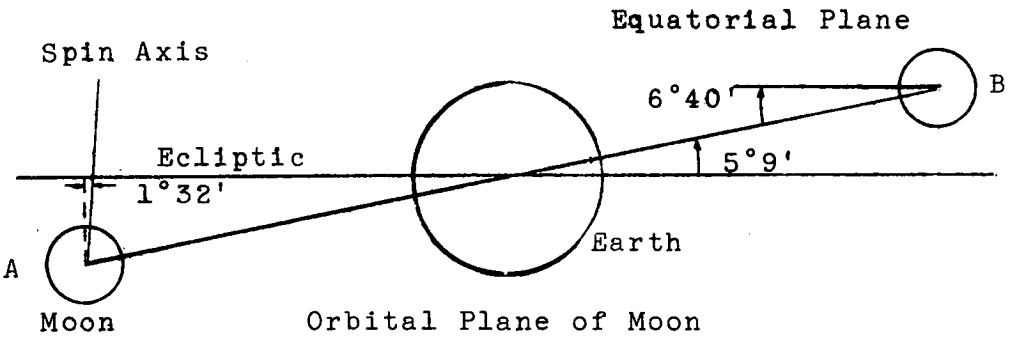

Figure 1

Orientation of the Lunar Equatorial Plane with Respect to the Lunar Orbit Plane.

which at each instant of time is tangent to the satellite orbit at the point occupied by the satellite. Hence, as the satellite moves along its path the orbital elements of the osculating ellipse are constantly varying with time. The rate at which they vary depends on the magnitude of the perturbing force. The limiting case of zero perturbing force results in simple two-body motion.

In the case of lunar satellites the principal perturbing forces are:

(1) Triaxality of the Moon

(2) Earth's gravity field

(3) Sun's gravity field

(4) Gravity fields of the planets

(5) Solar radiation pressure (important only for low density satellites).

The relative importance of these perturbing factors depends on the type of satellite and the nature of its orbit.

The perturbing force for this study is obtained after making the following assumptions:

(1) The Moon is a triaxial ellipsoid of uniform mass distribution.

(2) The Earth is a point mass which moves in an elliptical orbit about the Earth-Moon mass center. The initial orientation of the

Earth-Moon system is determined from a truncated set of Brown's ephemeris equations. The subsequent motion of the Earth relative to the Moon is approximated by elliptical two-body motion. For the time periods of interest here this is a reasonable assumption.

(3) The lunar equatorial plane is inclined 6°40' to the Earth-Moon orbit plane.

(4) The mass of the satellite is negligible.

(5) The effects of the Sun are neglected since it has been shown (Reference 10) that they are on the order of 0.005 times the effects of the perturbations due to the Earth.

(6) All other perturbing effects are neglected.

These assumptions must be incorporated into a system of perturbation equations which describe the time rates of change of the orbit elements of the osculating ellipse. Before considering these equations, the ephemeris equations for locating the relative Earth-Moon position for the selected epoch date will be discussed.

C. Earth-Moon Ephemeris Equations

In view of the current schedule for project Apollo, the epoch date of January 29, 1970, was chosen for this study. At that time the Moon will be entering its

third quarter, and lighting will be favorable for a lunar landing. Since published ephemeris data for the Moon are not available this far in advance, approximate equations based on Brown's theory were used to establish the relative Earth-Moon position for this epoch date.

In 1920, E. W. Brown published a set of tables of motion of the Moon which have subsequently been used to describe the lunar ephemeris. These tables are the result of some 1,500 separate terms which account for the perturbation in the Moon's motion due to such effects as the presence of the Sun and planets and the ellipsoidal figure of the Earth.

A truncated form of Brown's series expansions may be used to determine an approximate position of the Moon as a function of time. The equations used in this analysis to approximate the Moon's position were taken from the appendix of Reference 1 and may also be found in Reference 8, pages 109-145.

Figure 2 shows the geometry of the Moon relative to the Earth. The geocentric mean longitude of the Moon, its perigee, and its node are represented by L_m, $\tilde{\omega}_m$, and Ω_m respectively and are measured in the plane of the ecliptic. The symbols L_s and $\tilde{\omega}_s$ are the geocentric mean longitudes of the Sun and of its perigee. Further define

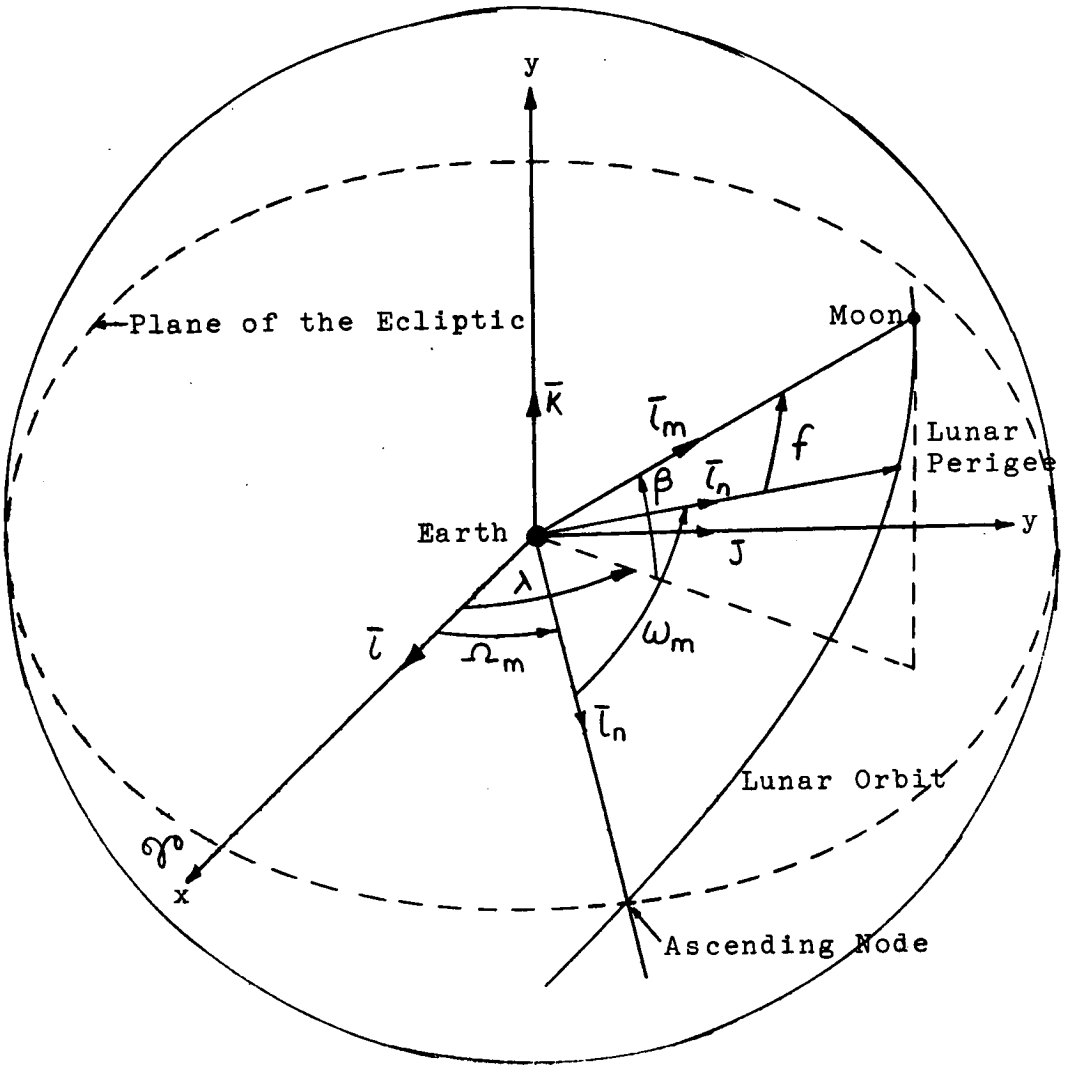

Figure 2

Geometry of the Earth-Moon System.

$$A' = L_m - L_s \qquad C' = L_s - \tilde{\omega}_s$$

$$B' = L_m - \tilde{\omega}_m \qquad D' = L_m - \Omega_m \quad .$$

Now, if λ is the true longitude of the Moon measured in the plane of the ecliptic and β is the true latitude above the plane of the ecliptic, then $\lambda - L_m$ and β can be expressed by sums of periodic terms whose arguments are algebraic sums of multiples of the four angles A', B', C', and D'.

In this approximation the expressions for longitude and latitude include only the effects of solar perturbations on the two-body motion of the Earth-Moon system, i.e., the effect of the planets and the oblateness of the Earth are neglected. Furthermore, only terms whose coefficients exceed 60 seconds of an arc are retained. The expressions in seconds of arc are as follows:

$$\begin{aligned}
\text{Longitude} = L_m &+ 22{,}639.500 \sin B' - 4{,}586.426 \sin (B' - 2A') \\
&+ 2{,}369.902 \sin 2A' + 769.016 \sin 2B' \\
&- 668.111 \sin C' - 411.608 \sin 2D' \\
&- 211.656 \sin (2B' - 2A') \\
&- 205.962 \sin (B' + C' - 2A') \\
&- 125.154 \sin A' + 191.953 \sin (B' + 2A') \\
&- 165.145 \sin (C' - 2A') \\
&+ 147.693 \sin (B' - C') \\
&- 109.667 \sin (B' + C')
\end{aligned}$$

$$\begin{aligned}\text{Latitude} = {} & 18{,}461.480 \sin D' + 1{,}010.180 \sin (B' + D') \\ & - 999.695 \sin (D' - B') - 623.658 \sin (D' - 2A') \\ & + 117.262 \sin (D' + 2A') \\ & + 199.485 \sin (D' + 2A' - B') \\ & - 166.577 \sin (B' + D' - 2A') \\ & + 61.913 \sin (2B' + D') \ .\end{aligned}$$

The fundamental arguments in these equations are functions of time and are given in Brown's "Tables of Motion of the Moon." The equations for these quantities are:

$$L_m = 270°26'11''.71 + 1{,}336^r\ 307°53'26''.06\ t_c + 7.14''\, t_c^2 + 0''.0068\ t_c^3$$

$$\tilde{\omega}_m = 334°19'46''.40 + 11^r\ 109°02'02''.52\ t_c - 37''.17\ t_c^2 - 0''.045\ t_c^3$$

$$\Omega_m = 259°10'59''.79 - 5^r\ 134°08'31''.23\ t_c + 7''.48\ t_c^2 + 0''.008\ t_c^3$$

$$A' = 350°44'23''.67 + 1{,}236^r\ 307°07'17''.93\ t_c + 6''.05\ t_c^2 + 0''.0068\ t_c^3$$

$$B' = 296°06'25''.31 + 1{,}325^r\ 198°51'23''.54 t_c + 44''.31\ t_c^2 + 0''.0518\ t_c^3$$

$$C' = 358°28'33''.00 + 99^r 359°02'59''.10\ t_c - 0''.54\ t_c^2 - 0''.0120\ t_c^3$$

$$D' = 11°15'11''.92 + 1,342^r 82°1'57''.29\ t_c - 0''.34\ t_c^2 - 0''.0012\ t_c^3 \ .$$

Here t_c is the time in Julian centuries which has elapsed since the epoch, January 0, 1900. On this date 2,415,020 Julian days have elapsed, hence

$$t_c = \frac{\text{Julian day no. - 2,415,020}}{36,525} \ .$$

It has been shown in Reference 1 that these equations are accurate to just over 3 minutes of an arc in longitude and 2 minutes in latitude.

In order to calculate the position of the Moon, let x,y,z in Figure 2 be a geocentric rectangular ecliptic-oriented coordinate system with the x axis directed toward the vernal equinox of January 0, 1900. Then, if $\bar{i},\bar{j},\bar{k}$ are unit vectors in the directions of the coordinate axes, the unit vector in the direction of the Moon, $\bar{i}_m$, is given by

$$\bar{i}_m = \cos\beta \cos\lambda\ \bar{i} + \cos\beta \sin\lambda\ \bar{j} + \sin\beta\ \bar{k} \ .$$

Further, the unit vectors, $\bar{i}_n$ and $\bar{i}_\xi$, in the directions of the ascending node and the lunar perigee are given in the form

$$\bar{i}_n = \cos \Omega_m \bar{i} + \sin \Omega_m \bar{j}$$

$$\bar{i}_\xi = (\cos \Omega_m \cos \omega_m - \sin \Omega_m \sin \omega_m \cos i_e)\bar{i}$$
$$+ (\sin \Omega_m \cos \omega_m + \cos \Omega_m \sin \omega_m \cos i_e)\bar{j}$$
$$+ (\sin \omega_m \sin i_e)\bar{k}$$

where i_e is the inclination of the lunar orbit to the ecliptic and ω_m is the longitude of lunar perigee measured from the ascending node. From Figure 2, it is seen that

$$\cos i_e = \frac{|\bar{i}_n \times \bar{i}_m \cdot \bar{k}|}{\bar{i}_n \times \bar{i}_m}$$

$$= \frac{\cos \beta \sin |\lambda - \Omega_m|}{\sqrt{1 - \cos^2\beta \cos^2(\lambda - \Omega_m)}}$$

and the true anomaly, f, of the Moon is

$$\cos f = \bar{i}_\xi \cdot \bar{i}_m$$

$$= \cos \beta \cos \omega_m \cos (\lambda - \Omega_m)$$
$$+ \cos \beta \sin \omega_m \cos i_e \sin (\lambda - \Omega_m)$$
$$+ \sin \beta \sin \omega_m \sin i_e \quad .$$

The sign of f is the same as the sign of $\bar{i}_\xi \times \bar{i}_m \cdot \bar{k}$, so that

$$\sin f = \text{sign}\,[\cos \omega_m \sin(\lambda - \Omega_m) - \sin \omega_m \cos i_e \cos(\lambda - \Omega_m)]\sqrt{1 - \cos^2 f}\,.$$

On January 29, 1970, the epoch chosen for this study, the quantities defining the Earth-Moon orientation are:

Julian Day number = 2,440,616

$L_m = 213.488°$

$\omega_m = 305.823°$

$\Omega_m = 343.776°$

$\lambda = 205.928°$

$\beta = -3.601°$

$f = 260.229°$

$D = 265.153°$.

The elongation of the Moon, D, is the angle measured in the ecliptic, from the Earth-Sun line, westward, to the projection of the Earth-Moon line on the ecliptic.

For this analysis the above set of geocentric orientation angles must be transformed to the selenocentric

inertial coordinate system described in the next section. However, transformation is simplified by the fact that the x axis of the selenocentric system is chosen to be parallel to the line of nodes of the geocentric system.

After establishment of the initial orientation, subsequent motion of the Earth-Moon system is approximated by ideal two-body motion. In Reference 12 on pages 32-53, derivations of the two-body equations used in this analysis are presented. The results are summarized below:

(1) $$E = M_o + e \sin M + \frac{e^2}{2} \sin 2M + \frac{e^3}{8} (3\sin 3M - \sin M) + \cdots$$

(2) $$\tan \frac{f}{2} = \left[\frac{1 + e}{1 - e}\right]^{\frac{1}{2}} \tan \frac{E}{2}$$

(3) $$\cos f = \frac{\cos E - e}{1 - e \cos E}$$

(4) $$r_e = \frac{a(1 - e^2)}{1 + e \cos f} \quad .$$

Here a is the semi-major axis, e, the eccentricity, and f, the true anomaly of the Earth-Moon orbit. The mean anomaly, M, is the product of the mean angular velocity of the Moon about the Earth, ω_e, and the time elapsed since previous

perigee passage. The relationship for E, the eccentric anomaly, (Equation 1) is a series expansion of Kepler's Equation

$$E - e \sin E = M \quad . \tag{5}$$

Average values for the Earth-Moon orbit elements are

$$a = 384{,}422 \text{ KM}$$

$$e = 0.0549$$

$$\omega_e = 0.266507564 \times 10^{-5} \text{ rad/sec}$$

D. Coordinate System

Prior to developing the perturbation equations, the coordinate systems employed for this analysis will be described (see Figure 3).

(1) Selenocentric "Inertial" Coordinate System (x,y,z). Here the word "inertial" is used to indicate that the coordinate system does not rotate but translates only. This system has its origin at the Moon's center of mass. The x axis lies along the intersection of the lunar equatorial plane and the Earth-Moon orbit plane and is directed toward the ascending node of the Earth's orbit

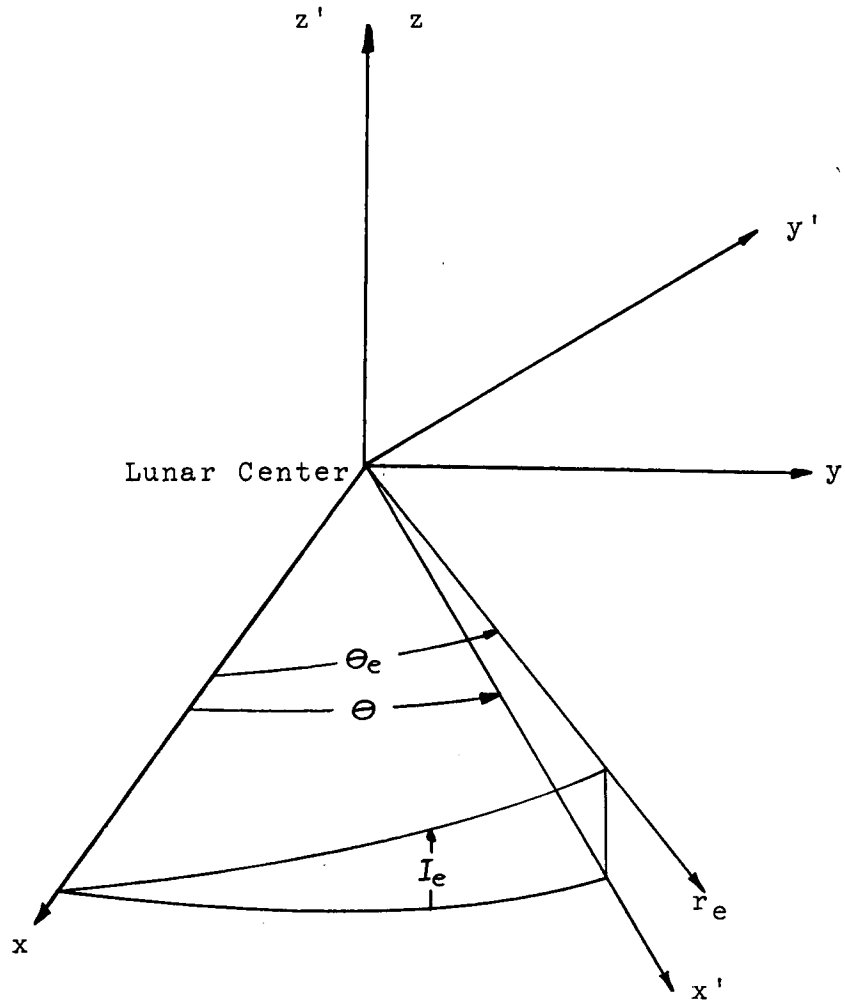

Figure 3.

Selenocentric Coordinate Systems.

relative to the Moon. The z axis is directed along the Moon's spin axis, and the y axis lies in the equatorial plane so as to form a right hand triad. The positive direction of these axes is shown in Figure 3.

(2) Body Fixed Selenocentric Coordinate System (x',y',z'). The x',y',z' coordinate system corresponds to the principle axes of inertia and forms a right hand triad. The x',y' axes lie in the lunar equatorial plane. The x' axis is directed toward the Earth, and the z' axis coincides with the Moon's spin axis. This coordinate system rotates with a constant angular velocity equal to the Moon's spin rate.

The angle θ is measured in the lunar equatorial plane and is the orientation angle between the x,y,z and x',y',z' axes systems ($0 \leq \theta \leq 360°$). The angle θ_e between the inertial x axis and r_e, the Earth's radius vector, is measured in the Earth-Moon orbit plane ($0 \leq \theta_e \leq 360°$). The relevant expressions are:

$$\theta_e = f + \theta_o$$

$$\theta = M + \arctan(\cos I_e \tan \theta_o)$$

where f is the true anomaly, M is the mean anomaly, and

θ_0 is the phase angle between the x axis and perigee of the Earth's orbit relative to the Moon.

E. Perturbation Equations

Fundamentally, six constants or orbit elements are required to describe a satellite's orbit, four to describe the orbit in plane and two to orient it with respect to the coordinate system. The orbit in plane is described by

P : semi-latus rectum

e : eccentricity

ω : argument of pericenter

t_p : time of perigee passage .

The orbit plane is oriented with reference to the coordinate system by

Ω : longitude of ascending node

I : inclination of the orbital plane to the equatorial plane .

For circular orbits, ω and t_p have no significance since pericenter is undefined. Since in this study

circular orbits will be of primary interest, these quantities will not be directly considered.

Generally, Lagrange's Planetary Equations are used to describe the time rates of change of the orbit elements (Reference 13), however, singularities arise in this set of equations for zero eccentricity. To avoid this difficulty, an alternate set of equations described in Reference 14 has been adopted for this study. Since their derivation is not readily available in the literature, it will be presented here.

The x,y,z axis system in Figure 4 is the same selenocentric inertial system discussed previously. The unit vectors $\bar{i},\bar{j},\bar{k}$ lie along the x,y,z axis respectively. Two vector combinations of $\bar{r}$, the radius, and $\bar{V}$, the velocity, which will be used in this analysis are the angular momentum and eccentricity vector, defined as:

$$\bar{h} = \bar{r} \times \bar{V} \tag{6}$$

$$\bar{e} = \frac{\bar{V} \times \bar{h}}{\mu_m} - \bar{\epsilon}_r \ . \tag{7}$$

Here a subscripted $\bar{\epsilon}$ is an unit vector in the subscript direction, and μ_m is the Moon's gravitational constant.

The vector $\bar{e}$ lies along the major axis always directed toward periselene.

In Figure 4, $\bar{\epsilon}_\Omega$ is an unit vector lying along the line of intersection of the instantaneous orbit plane and the Moon's equatorial plane and directed toward the instantaneous ascending node. The inclination angle of the orbital plane, I, is measured from 0° to 180°, "right handed" with respect to $\bar{\epsilon}_\Omega$. The angles u and ω are measured from 0° to 360° in the orbital plane from the ascending node to $\bar{r}$ and $\bar{e}$ respectively. The longitude of the ascending node, Ω, is measured from 0° to 360° in the equatorial plane from the x axis to $\bar{\epsilon}_\Omega$.

To determine the transformations between $\bar{r}$ and $\bar{V}$ and h, e, ω, u, Ω, and I, we first write $\bar{r}$ and $\bar{V}$ in terms of $\bar{\epsilon}_r$ and $\bar{\epsilon}_i$, a lateral unit vector in the $\bar{r}$, $\bar{V}$ plane ($\bar{\epsilon}_i = \bar{\epsilon}_h \times \bar{\epsilon}_r$). The radius vector is simply $r\bar{\epsilon}_r$, in which the magnitude of r may be found by dotting each side of Equation (7) with $\bar{r}$ and introducing Equation (6). That is

$$\bar{r} \cdot [\bar{e} + \bar{\epsilon}_r] = \bar{r} \cdot \frac{\bar{V} \times \bar{h}}{\mu_m} = \frac{\bar{r} \times \bar{V} \cdot \bar{h}}{\mu_m} = \frac{\bar{h} \cdot \bar{h}}{\mu_m}$$

$$r[e \cos (u - \omega) + 1] = \frac{h^2}{\mu_m}$$

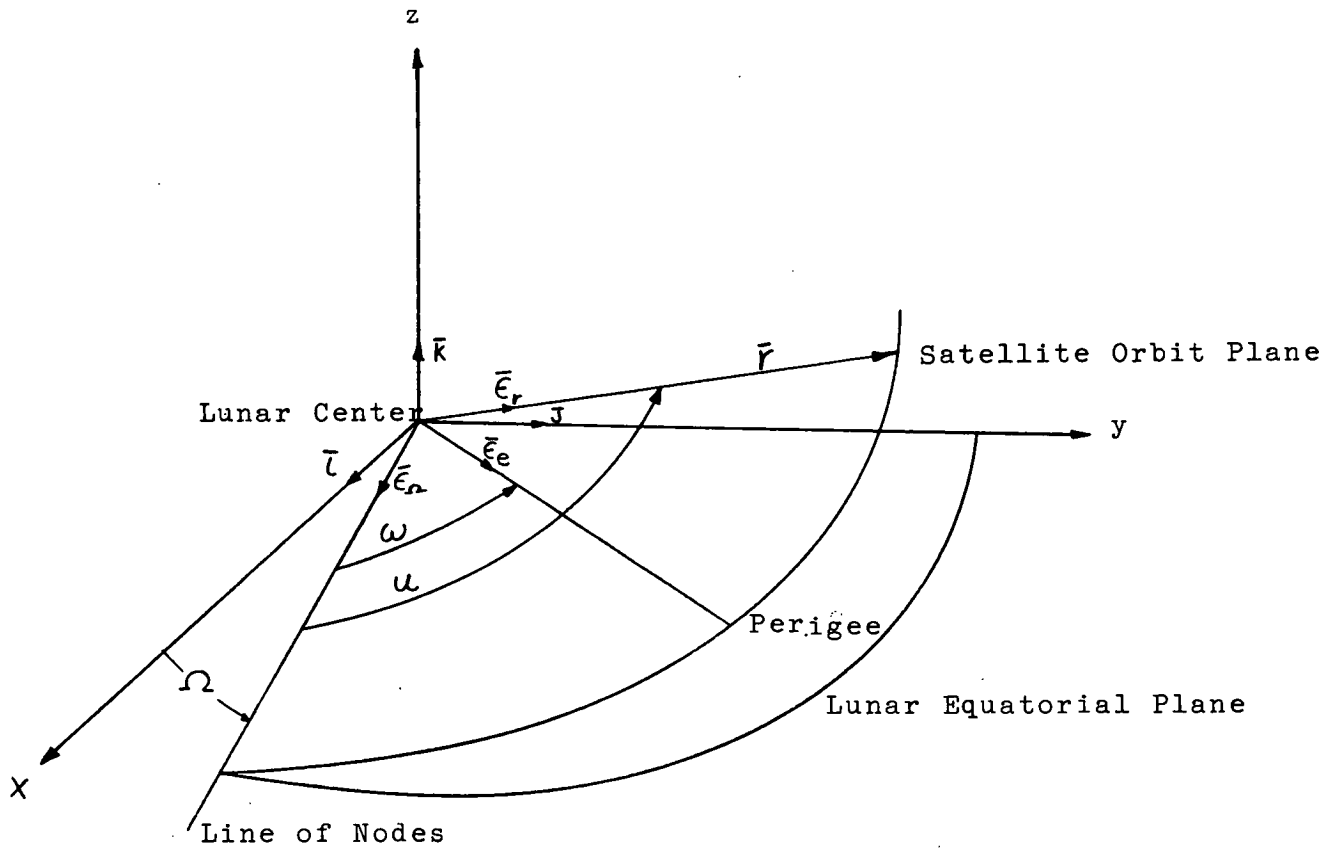

Figure 4.

Satellite Position with Respect to Selenocentric Inertial Coordinate System.

$$(8) \qquad \bar{r} = \frac{\frac{h^2}{\mu_m}\bar{\epsilon}_r}{1 + e \cos (u - \omega)} .$$

$\bar{V}$ is solved for from Equation (7) by crossing each side with $\bar{h}$

$$\bar{h} \times [\bar{e} + \bar{\epsilon}_r] = \bar{h} \times \frac{\bar{V} \times \bar{h}}{\mu_m}$$

$$\bar{h} \times \{e[\cos (u - \omega)\bar{\epsilon}_r - \sin (u - \omega)\bar{\epsilon}_i] + \bar{\epsilon}_r\}$$

$$= \frac{(\bar{h} \cdot \bar{h})\bar{V}}{\mu_m} - \frac{(\bar{h} \cdot \bar{V})\bar{h}}{\mu_m} = \frac{h^2}{\mu_m} \bar{V}$$

$$(9) \qquad \bar{V} = \frac{\mu_m}{h}\{[e \cos (u - \omega) + 1]\bar{\epsilon}_i + e \sin (u - \omega)\bar{\epsilon}_r\} .$$

The following terms will now be defined to further simplify computations and to eliminate the small eccentricity restriction of Lagrange's Planetary Equations:

$$P = \frac{h^2}{\mu_m} , \qquad A = e \cos \omega , \qquad B = e \sin \omega .$$

Substituting these expressions into Equations (8) and (9) yields

$$\bar{r} = \frac{P\bar{\epsilon}_r}{1 + e \cos (u - \omega)}$$

which may be written as

$$\bar{r} = \frac{P\bar{\epsilon}_r}{1 + A \cos u + B \sin u} \tag{10}$$

and

$$\bar{V} = \frac{\mu_m}{h} [(1 + A \cos u + B \sin u)\bar{\epsilon}_i + (A \sin u - B \cos u)\bar{\epsilon}_r] . \tag{11}$$

The reverse transformation is the determination of the defined quantities when given $\bar{r}$ and $\bar{V}$. These quantities follow directly from the definition of the variables:

$$\bar{h} = \bar{r} \times \bar{V} , \quad P = \frac{\bar{h} \cdot \bar{h}}{\mu_m}, \quad \bar{\epsilon}_h = \frac{\bar{h}}{+\sqrt{\bar{h} \cdot \bar{h}}},$$

$$\bar{\epsilon}_r = \frac{\bar{r}}{+\sqrt{\bar{r} \cdot \bar{r}}}, \quad \bar{\epsilon}_\Omega = \frac{\bar{k} \times \bar{\epsilon}_h}{\sin I} , \quad A = \bar{\epsilon}_\Omega \cdot \bar{e} ,$$

$$B = \bar{\epsilon}_\Omega \times \bar{e} \cdot \bar{\epsilon}_h , \quad \cos I = \bar{\epsilon}_h \cdot \bar{k} , \quad 0 \leq I \leq 180^\circ \tag{12}$$

$$\cos \Omega = \bar{\epsilon}_\Omega \cdot \bar{i} , \quad \sin \Omega = \bar{\epsilon}_\Omega \cdot \bar{j} , \quad 0 \leq \Omega \leq 360^\circ$$

$$\cos u = \bar{\epsilon}_\Omega \cdot \bar{\epsilon}_r \ , \quad \sin u = \bar{\epsilon}_\Omega \times \bar{\epsilon}_r \cdot \bar{\epsilon}_h \ ,$$

$$0 \leq u \leq 360^\circ \ .$$

The sets of equations for Ω and u are solved in pairs to determine the proper quadrant for the angle.

Now consider the equation of motion

$$\frac{d\bar{V}}{dt} = \frac{\overline{\text{force}}}{M}$$

or in alternate form

$$\frac{d\bar{V}}{dt} = \bar{F} - \frac{\mu_m \bar{r}}{r^3} \tag{13}$$

where M is the mass of the satellite.

In the alternate form it may be seen that $\bar{F}$ is the perturbing force since the case for $\bar{F} = 0$ corresponds to central force field motion.

Equation (13) along with Equation (12) can be transformed into the derivatives of the six orbit elements, thus forming the perturbation equations.

Since Equation (12) expresses the orbital elements most directly as functions of $\bar{h}$ and $\bar{e}$, their derivatives are facilated with expressions for $\dot{\bar{h}}$ and $\dot{\bar{e}}$.

$$\dot{\bar{h}} = \dot{\bar{r}} \times \bar{V} + \bar{r} \times \dot{\bar{V}}$$

From Equation (13), it follows that

$$\dot{\bar{h}} = \bar{V} \times \bar{V} + \bar{r} \times (\bar{F} - \frac{\mu_m \bar{r}}{r^3}) = \bar{r} \times \bar{F} \quad . \tag{14}$$

The derivative of any unit vector $\bar{\epsilon}_a$ is

$$\dot{\bar{\epsilon}}_a = \frac{d(\frac{\bar{a}}{a})}{dt} = \frac{1}{a} \dot{\bar{a}} - \frac{\bar{a}}{a^2} \dot{a} = \frac{1}{a^3} [(\bar{a} \cdot \bar{a})\dot{\bar{a}} - \bar{a}(\bar{a} \cdot \dot{\bar{a}})]$$

$$= \frac{1}{a^3} (\bar{a} \times \dot{\bar{a}}) \times \bar{a} \quad .$$

Using this expression, it follows from Equation (7) and Equation (14) that

$$\mu_m \dot{\bar{e}} = \dot{\bar{V}} \times \bar{h} + \bar{V} \times \dot{\bar{h}} - \mu_m \dot{\bar{\epsilon}}_r$$

$$= \dot{\bar{V}} \times \bar{h} + \bar{V} \times (\bar{r} \times \bar{F}) - \frac{\mu_m}{r^3} (\bar{r} \times \bar{V}) \times \bar{r}$$

$$= (\dot{\bar{V}} + \frac{\mu_m \bar{r}}{r^3}) \times \bar{h} + \bar{V} \times (\bar{r} \times \bar{F})$$

$$= \bar{F} \times (\bar{r} \times \bar{V}) + \bar{V} \times (\bar{r} \times \bar{F}) \quad . \tag{15}$$

The derivative of P, the semi-latus rectum, becomes

$$\dot{P} = \frac{d}{dt}\left(\frac{\bar{h} \cdot \bar{h}}{\mu_m}\right) = \frac{2\bar{h}}{\mu_m} \cdot \dot{\bar{h}} = \frac{2\bar{h}}{\mu_m} \cdot \bar{r} \times \bar{F}$$

$$= \frac{2\bar{h}}{\mu_m} \times \bar{r} \cdot \bar{F} = \frac{2hr}{\mu_m} (\bar{\epsilon}_i \cdot \bar{F}) \quad . \tag{16}$$

From Equation (12) the derivative of I is found to be

$$-\sin I \, \dot{I} = \frac{d}{dt} (\bar{\epsilon}_h \cdot \bar{k}) = \frac{1}{h^3} (\bar{h} \times \dot{\bar{h}}) \times \bar{h} \cdot \bar{k}$$

$$= \frac{1}{h^3} (\bar{h} \times \dot{\bar{h}}) \cdot \bar{h} \times \bar{k}$$

$$= \frac{1}{h^3} (\bar{h} \times \dot{\bar{h}}) \cdot (-\bar{\epsilon}_\Omega h \sin I)$$

$$\dot{I} = \frac{\bar{\epsilon}_\Omega \times \bar{h}}{h^2} \cdot \dot{\bar{h}} = \frac{\bar{\epsilon}_\Omega \times \bar{\epsilon}_h}{h} \cdot (\bar{r} \times \bar{F})$$

$$= \frac{r}{h} (\bar{\epsilon}_\Omega \times \bar{\epsilon}_h) \times \bar{\epsilon}_r \cdot \bar{F}$$

$$\dot{I} = \frac{r}{h} \cos u \, (\bar{\epsilon}_h \cdot \bar{F}) \quad . \tag{17}$$

Since the remaining orbit elements are expressed in terms of ϵ_Ω, $\dot{\bar{\epsilon}}_\Omega$ will be introduced now, i.e.,

$$\dot{\bar{\epsilon}}_\Omega = \frac{d}{dt} \frac{(\bar{k} \times \bar{h})}{h \sin I} = \frac{\bar{k}}{h \sin I} \times \dot{\bar{h}} - \frac{\bar{k} \times \bar{h}}{h^2 \sin^2 I} \frac{d}{dt} (h \sin I)$$

$$= \frac{\bar{k} \times \dot{\bar{h}}}{h \sin I} - \frac{\bar{\epsilon}_\Omega}{h \sin I} \frac{d}{dt}(\bar{k} \times \bar{h} \cdot \bar{\epsilon}_\Omega) \ .$$

The derivative of an unit vector is perpendicular to the unit vector, hence $\bar{k} \times \bar{h} \cdot \dot{\bar{\epsilon}}_\Omega = 0$, and

$$\dot{\bar{\epsilon}}_\Omega = \frac{1}{h \sin I} [\bar{k} \times \dot{\bar{h}} - \bar{\epsilon}_\Omega(\bar{k} \times \dot{\bar{h}} \cdot \bar{\epsilon}_\Omega)]$$

$$= \frac{[\bar{\epsilon}_\Omega \times (\bar{k} \times \dot{\bar{h}})]}{h \sin I} \times \bar{\epsilon}_\Omega \ . \tag{18}$$

Then from Equation (12) and Figure 4

$$- \sin \Omega \ \dot{\Omega} = \frac{d}{dt} (\bar{\epsilon}_\Omega \cdot \bar{i}) = \frac{\bar{\epsilon}_\Omega}{h \sin I} \times (\bar{k} \times \dot{\bar{h}}) \cdot \bar{\epsilon}_\Omega \times \bar{i}$$

$$= \frac{\bar{\epsilon}_\Omega}{h \sin I} \times (\bar{k} \times \dot{\bar{h}}) \cdot (-\bar{k} \sin \Omega)$$

$$\dot{\Omega} = \frac{\bar{k} \times \bar{\epsilon}_\Omega}{h \sin I} \cdot \bar{k} \times \dot{\bar{h}}$$

$$= \frac{\bar{\epsilon}_\Omega}{h \sin I} \cdot (\bar{r} \times \bar{F})$$

$$\dot{\Omega} = \frac{r \sin u}{h \sin I} (\bar{\epsilon}_h \cdot \bar{F}) \ . \tag{19}$$

Also,

$$- \sin u \, \dot{u} = \bar{\epsilon}_\Omega \cdot \dot{\bar{\epsilon}}_r + \dot{\bar{\epsilon}}_\Omega \cdot \bar{\epsilon}_r$$

$$= \frac{\bar{\epsilon}_\Omega}{r^3} \cdot (\bar{r} \times \bar{V}) \times \bar{r}$$

$$+ \frac{[\bar{\epsilon}_\Omega \times (\bar{k} \times \dot{\bar{h}})] \cdot [\sin u \, \bar{\epsilon}_h]}{h \sin I} .$$

Using the previous relationship for $\dot{\Omega}$ it can be seen that

$$\frac{[\bar{\epsilon}_\Omega \times \bar{k} \times \dot{\bar{h}}]}{h \sin I} = \dot{\Omega}\bar{k}$$

since it must be in the $\pm \bar{k}$ direction. It follows then that

$$\dot{u} = \frac{h}{r^2} - \dot{\Omega} \cos I .$$

Finally, from Equations (12) and (18)

$$\dot{A} = \dot{\bar{\epsilon}}_\Omega \cdot \bar{e} + \bar{\epsilon}_\Omega \cdot \dot{\bar{e}}$$

$$= \dot{\Omega}\bar{k} \cdot \bar{\epsilon}_\Omega \times \bar{e} + \bar{\epsilon}_\Omega \cdot \dot{\bar{e}}$$

$$= B\dot{\Omega} \cos I + \bar{\epsilon}_\Omega \cdot \bar{e}$$

$$\dot{B} = \dot{\bar{\epsilon}}_\Omega \cdot \bar{e} \times \bar{\epsilon}_h + \bar{\epsilon}_\Omega \times \dot{\bar{e}} \cdot \bar{\epsilon}_h$$

$$= - A\dot{\Omega} \cos I + \bar{\epsilon}_\Omega \cdot (\dot{\bar{e}} \times \bar{\epsilon}_h) .$$

Using Equations (8) and (9) for $\bar{r}$ and $\bar{V}$ and Equation (15) for $\dot{\bar{e}}$, the following expressions can be obtained

$$\dot{A} = B\dot{\Omega} \cos I + \frac{r}{h} \{ \psi \sin u \bar{\epsilon}_r + [A + (1 + \psi) \cos u] \bar{\epsilon}_i \} \cdot \bar{F} \tag{20}$$

$$\dot{B} = - A\dot{\Omega} \cos I + \frac{r}{h} \{ - \psi \cos u \bar{\epsilon}_r + [B + (1 + \psi) \sin u] \bar{\epsilon}_i \} \cdot \bar{F} \quad . \tag{21}$$

The collected results, called the perturbation equations, are the following set of first order nonlinear differential equations:

$$\dot{P} = \frac{2hr}{\mu_m} (\bar{\epsilon}_i \cdot \bar{F})$$

$$\dot{I} = \frac{r}{h} \cos u \, (\bar{\epsilon}_h \cdot \bar{F})$$

$$\dot{A} = B\dot{\Omega} \cos I + \frac{r}{h} \{ \psi \sin u \bar{\epsilon}_r + [A + (1 + \psi) \cos u] \bar{\epsilon}_i \} \cdot \bar{F}$$

$$\dot{B} = - A\dot{\Omega} \cos I + \frac{r}{h} \{ - \psi \cos u \bar{\epsilon}_r + [B + (1 + \psi) \sin u] \bar{\epsilon}_i \} \cdot \bar{F} \tag{22}$$

$$\dot{\Omega} = \frac{r}{h} \frac{\sin u}{\sin I} (\bar{\epsilon}_h \cdot \bar{F})$$

$$\dot{u} = \frac{h}{r^2} - \dot{\Omega} \cos I$$

$$= \frac{h}{r^2} \left[1 - \frac{\sin u \cos I}{\sin I} \frac{r^3}{h^2} (\bar{\epsilon}_h \cdot \bar{F})\right] .$$

Where

$$\psi = 1 + A \cos u + B \sin u ,$$

it is convenient to define

$$R = \bar{\epsilon}_r \cdot \bar{F} , \qquad C = \bar{\epsilon}_i \cdot \bar{F} , \qquad W = \bar{\epsilon}_h \cdot \bar{F} .$$

The expressions R, C, and W are the components of the perturbing acceleration in the radial, circumferential, and normal directions respectively. They will be used in a subsequent discussion. An expression for the perturbing acceleration now will be developed.

F. Potential Energy Function

It is known from observations over the past one hundred years that the Moon can be approximated as a homogeneous triaxial ellipsoid, i.e., the Moon has three

principle axes of inertia. To accurately simulate the motion of a satellite this triaxialty must be considered when defining the lunar gravitational potential. For a derivation of the potential energy function of a triaxial ellipsoid, see Reference 2, pages 115-125.

The gravitational potential per unit mass of a point P at a distance r from the center of mass O of any rigid body of mass M is

$$(23) \qquad V_m = -G\left(\frac{M}{r} + \frac{A_1 + B_1 + C_1 - 3I'}{2r^3}\right) + O\left(\frac{1}{r^4}\right) .$$

Where G is the universal gravitational constant, I' is the moment of inertia of M about the line segment OP, and A_1, B_1, C_1 are moments of inertia about the three principle axes of inertia (x',y',z'). Also, in the principle axis system,

$$(24) \qquad I' = A_1\left(\frac{x'}{r}\right)^2 + B_1\left(\frac{y'}{r}\right)^2 + C_1\left(\frac{z'}{r}\right)^2$$

where

$$r^2 = x'^2 + y'^2 + z'^2 .$$

The higher order terms in $1/r^4$ will be neglected.

The Earth will be treated as a point mass for this analysis since the distance between the Earth and the satellite remains large. Accordingly, the Earth's gravitational potential is approximated by the following expression

$$(25) \qquad V_e = GM_e\left[\frac{1}{r_{es}} - \frac{xx_e + yy_e + zz_e}{r_e^3}\right] \quad .$$

The total potential energy function is then the sum of Equations (23) and (25). Using this relationship for the total potential function, V_t, the equations of motion for the satellite are given in Reference 7 as:

$$(26) \qquad \ddot{X} = \frac{GM_e}{r_{es}^3}(x_e - x) - \frac{GM_e}{r_e^3} x_e + G\left[H \frac{x}{r} - \frac{3}{r^5}\left(A_1 a_{11} x' + B_1 a_{21} y' + C_1 a_{31} z'\right)\right]$$

$$(27) \qquad \ddot{Y} = \frac{GM_e}{r_{es}^3} (y_e - y) - \frac{GM_e}{r_e^3} y_e + G\left[H \frac{y}{r} - \frac{3}{r^5}\left(A_1 a_{12} x' + B_1 a_{22} y' + C_1 a_{32} z'\right)\right]$$

$$(28) \qquad \ddot{Z} = \frac{GM_e}{r_{es}^3} (z_e - z) - \frac{GM_e}{r_e^3} z_e + G\left[H \frac{z}{r} - \frac{3}{r^5}\left(A_1 a_{13} x' + B_1 a_{23} y' + C_1 a_{33} z'\right)\right] .$$

The radius vector of the satellite, r, is given by:

$$r = P/(1 + A \cos u + B \sin u) \ .$$

The components of the satellite's position vector are:

$$x = r(\cos u \cos \Omega - \sin u \sin \Omega \cos I)$$

$$y = r(\cos u \sin \Omega + \sin u \cos \Omega \cos I)$$

$$z = r(\sin u \sin I) \ .$$

From Figure 3 the expressions for x_e, y_e, z_e are:

$$x_e = r_e \cos \theta_e$$

$$y_e = r_e \sin \theta_e \cos I_e$$

$$z_e = r_e \sin \theta_e \sin I_e \ .$$

The a_{ij} are direction cosines which define the transformation between the inertial (x,y,z) coordinate system and the principle (x',y',z') axis system. The transformation matrix [A] is given by:

$$[A] = \begin{bmatrix} \cos \theta & \sin \theta & 0 \\ -\sin \theta & \cos \theta & 0 \\ 0 & 0 & 1 \end{bmatrix} \ .$$

The lunar force potential, H, is:

$$(29) \qquad H = \frac{M_m}{r^2} - \frac{3}{2}\frac{A_1 + B_1 + C_1}{r^4} + \frac{15}{2}\frac{1}{r^4}\left[A_1\left(\frac{x'}{r}\right)^2 + B_1\left(\frac{y'}{r}\right)^2 + C_1\left(\frac{z'}{r}\right)^2\right] .$$

In this study we are interested in only the perturbing accelerations which act on the satellites. Since A_1, B_1, and C_1 are zero for a spherical body of uniform mass distribution it is seen from Equation (29) that $\frac{M_m}{r^2}$ is the central force field contribution to the lunar force potential. If this term is removed, Equations (26), (27), and (28) will yield the components of the perturbing acceleration. The radial, circumferential, and normal components of the perturbing acceleration, R, C, and W, can be obtained from a coordinate transformation:

$$(30) \qquad R = \ddot{X}(\cos u \cos \Omega - \sin u \sin \Omega \cos I) + \ddot{Y}(\cos u \sin \Omega + \sin u \cos \Omega \cos I) + \ddot{Z}(\sin u \sin I)$$

$$(31) \qquad C = \ddot{X}(-\sin u \cos \Omega - \cos u \sin \Omega \cos I) + \ddot{Y}(-\sin u \sin \Omega + \cos u \cos \Omega \cos I) + \ddot{Z}(\cos u \sin I)$$

$$(32) \qquad W = \ddot{X}\,(\sin\Omega \sin I) - \ddot{Y}(\cos\Omega \sin I) + \ddot{Z}(\cos I) \quad .$$

Equations (22), (26), (27), (28), (30), (31), (32), and the two body equations of motion to approximate the motion of the Earth, Equations (1), (2), (3), and (4), were programmed for numerical solution with the CDC 1604 digital computer located in the computation center at The University of Texas.

III. COMPUTATIONAL PROCEDURE

The computations for this analysis were performed on the CDC 1604 digital computer utilizing a routine originally coded by D. S. Goddard to integrate Lagrange's Planetary Equations. This routine was revised to accommodate the equations and assumptions used for this study. A brief sketch of the routine will be given here; however, a more detailed description including a listing of the basic computer program is given in Reference 5.

The numerical integration was carried out using a partial double precision Adams-Moulton integration scheme with a Runge-Kutta starter. In this scheme an initial integration interval and one initial condition is supplied for each orbit element. The Runge-Kutta subroutine calculates three additional values. Control is then shifted to the Adams-Moulton subroutine which continues the integration and calculates the single step error. Then the single step error is checked against prescribed limits set by the user. If the error becomes too large the integration interval is halved, and control is returned to the

Runge-Kutta subroutine for new "starting values." If the error becomes too small the integration interval is doubled, and control remains with the Adams-Moulton subroutine. In this analysis it was found that an integration step size of 100 seconds resulted in an error within the bounds of 10^{-6} to 10^{-11}. A more complete description of this procedure is given in Reference 6 or in practically any numerical analysis text.

In order to facilitate integration, all input data and constants containing a length dimension were divided by 10^{-4} to force all independent variables to be of the same order of magnitude.

Two modes of output were employed for this study. One prints the values of the orbit elements at specified time intervals for 3 revolutions and shows the short term variations of the elements. The other prints only the local maximum and minimum values of the elements over a period of 80 revolutions. The minimum and maximum values of the elements are obtained by comparing the absolute value of each calculated point with the absolute value of the two previous points. When a local minimum or maximum value is detected, it is stored by the computer. These results can be used to obtain an envelope for the variation in the orbit elements over long periods of time.

On completion of the integration in both cases the results of each independent variable are arranged in column arrays. Each array is scanned for its maximum and minimum values, and then each element of the array is normalized. Hence, the maximum value of the array corresponds to one and the minimum value to zero. The normalized values of each orbit element are then plotted against time by the digital computer.

IV. RESULTS

A. Initial Values of Orbit Elements

As stated previously, this analysis deals with circular, low altitude satellite orbits of near equatorial inclinations. Table 1* presents initial input data for each of the twelve orbits considered here. Values of the orbit elements at the end of 80 revolutions are also shown, however, these will be discussed later.

Based on current speculation that the Apollo orbit will be circular, approximately 100 miles in altitude, and inclined at 170° to the lunar equator, initial altitudes of 50 miles (P = 1822.20 KM) and 150 miles (P = 1981.35 KM), and initial inclinations of 179.5°, 170°, 160°, .5°, 10°, and 20° were chosen for this study. For lack of any definitive information on the initial longitude of the ascending node for the Apollo orbit, it was chosen arbitrarily for this study to lie on the Earth-Moon line on the side of the Moon opposite the Earth.

Inclinations between 0 and 90° correspond to prograde orbits and inclinations of 90° through 180°

---

*See page 50.

correspond to retrograde orbits. Although the retrograde orbit has been confirmed for the Apollo mission, the prograde orbits were also considered to present a more complete picture of the orbital characteristics for near equatorial inclinations in this altitude range.

Subsequently, a specific orbit will be referred to as orbit type 1 through 12, depending on its initial parameters as shown in Table 1. Note that orbit types 1 through 6 are prograde, and orbit types 7 through 12 are retrograde.

B. Graphical Results*

1. Short Time Variations

The variation with time of the orbit elements for three (3) revolutions of orbit types 3, 4, 9, and 10 are presented in Figures 5 through 13. Rather than show the multitude of plots necessary to present the short time variations of the elements for all cases, only the results for inclinations of 10° and 170° are shown since these results are typical.

It is again pointed out that these are plots of the normalized values of the elements. Also note that the small normalizing difference used for this process results in a greatly enlarged scale. Consequently, a small change

---

*See pages 51 through 67.

in the value of the orbit element appears greatly exaggerated when plotted on this scale; however, this method of presenting the data facilitates analysis.

Both the maximum and minimum values of the orbit element are shown on each plot. The maximum and minimum values correspond to the ordinate values of one and zero respectively. Consequently, the value of the element at any point on the plot may be determined.

The plots of semi-latus rectum indicate that the time variation of P is practically independent of rotational direction for a given altitude over a period of three revolutions, i.e. the variation in P is identical for both direct and retrograde orbits of a given altitude.

It is seen from Figures 5, 7, 9, and 11 that the oscillations in the inclination of the retrograde orbits of a given altitude are displaced by 90° from those of the prograde orbits. The amplitude of the oscillations are greater also for the retrograde orbits. The time variation for a given inclination varies only slightly with altitude changes between 50 and 150 miles. All orbits experience a decrease in inclination over a period of three revolutions.

Figures 6, 8, 10, and 12, which present the time variation of the longitude of the ascending node, indicate

that Ω increases with time for the retrograde orbits and decreases with time for the prograde. This is to be expected since the component of the perturbing force normal to the satellite orbital plane, which causes the rotation of the line of nodes (Equation 22), will be in opposite directions for the two cases. It is noted also that the amplitude of the oscillations of Ω are considerably smaller than those of P or I. This effect is quite noticeable in the 80 revolutions plots.

Figures 6, 8, 10, and 12 indicate that the variation of eccentricity is practically independent of altitude or inclination for three revolutions. Figure 13, which presents e cos ω and e sin ω for orbit 10, is shown only to give an example of their variation with time since the argument of perigee, ω, is of little significance for near circular orbits.

The variation with time of the angle u, between the line of nodes and the satellite's radius vector, was found to be linear, indicating that the perturbing effects on it are negligible. Therefore, this angle will not be further considered.

2. Long Time Variations

Figures 14 through 19 present the envelope of variation which occurs in the values of the orbit elements for

orbit types 1 through 12 during a period of 80 satellite revolutions. The envelopes shown for each orbit are the locus of points of the maximum and minimum values of the oscillations of the orbit elements. These are once again normalized values so that while the actual magnitude of the change may be small, it may appear to be quite significant on the plot. In order to reduce the number of plots and show more readily the effects of inclination for a given orbit altitude, the plots of P, Ω, and e versus number of satellite revolutions are shown with three values of inclination on each plot. The maximum and minimum values of the elements are again shown on each plot as well as time ticks on the abscissa indicating time in days since injection into orbit. Figures 14 and 15 present P, Ω, and e for orbit types 1, 3, 5 and 2, 4, 6, respectively. Figures 17 and 18 show the variations in these elements for orbits 7, 9, 11 and 8, 10, 12 respectively. Since normalized values of inclination would appear as three straight lines if plotted in this manner, this element was plotted using altitude as the varying parameter. Figure 16 presents the three inclinations corresponding to the prograde orbits (orbit types 1 through 6), and Figure 19 presents the corresponding retrograde cases (orbit types 7 through 12).

It has been stated previously that the line of nodes progresses for retrograde and regresses for prograde orbits. This trend is again noted in Figures 14, 15, 17, and 18. The noticeable difference in each case between the results for the near equatorial inclinations, 0.5° and 179.5°, and those for the two orbits of greater inclinations are attributed to the effects of the Earth and the sin I term in the denominator of the relationship for $\dot{\Omega}$ in Equation 22. From the initial orientation of the Earth-Moon system it can be shown from spherical trigonometry that the latitude of the Earth with respect to the lunar equator is +4.48°. Moreover, this angle will remain positive for 10.5 additional days. Consequently, the component of the perturbing force of the Earth normal to the orbit plane will be in the same direction for all prograde orbits throughout 80 revolutions, but the sin I term will tend to increase the absolute magnitude of $\dot{\Omega}$ with decreasing inclination as shown in Figures 14 and 15. However, in the retrograde case the normal component of the Earth's perturbing force on the 179.5° inclination orbits will be directed opposite to that for the orbits inclined at 160° and 170° to the lunar equator. Furthermore, as shown in Figures 17 and 18 this factor is significant enough to reverse the effect of the decreasing

value of sin I and results in a smaller change in Ω for orbit types 7 and 8 than for orbit types 9, 10, 11, and 12. In brief the effect of the Earth is to cause a regression of the node for orbit types 1 through 8 and a progression for orbit types 9 through 12 throughout the time period considered here. This effect will be reversed when the latitude of the Earth with respect to the lunar equatorial plane becomes negative. The effects of the Earth are seen to increase with orbit altitude as would be expected.

The results for eccentricity indicate that this element oscillates in practically the same manner and with the same magnitude for all orbits. Harmonics which appear in Figures 14, 15, 17, and 18 begin after about 40 revolutions and continue throughout 80 revolutions. Figure 20 presents the variation with time of $e \cos \omega$ and $e \sin \omega$ for orbit 10.

The component of the perturbing force normal to the orbit plane also determines the direction of the change in inclination. Here, as in case of Ω, the effect of the Earth on orbit types 1 through 8 is opposite to the effect on orbit types 9 through 12. This phenomena is shown in Figures 16 and 19.

Table 1 presents the initial values of the orbit elements as well as their values after 80 revolutions. Since Ω is the only element which varies appreciably with the inclination, the final value of Ω is shown plotted against I for both orbit altitudes in Figure 21.

ORBIT TYPE	P-KM		I		Ω		e	
	INITIAL	FINAL	INITIAL	FINAL	INITIAL	FINAL	INITIAL	FINAL
1	1822.20	1821.78	0.5°	.4685°	222.276°	210.069°	0.0	.000234
2	1981.35	1980.93	0.5°	.4688°	222.276°	210.150°	0.0	.000236
3	1822.20	1821.79	10°	9.797°	222.276°	213.618°	0.0	.000229
4	1981.35	1980.93	10°	9.843°	222.276°	214.669°	0.0	.000232
5	1822.20	1821.81	20°	19.621°	222.276°	214.097°	0.0	.000223
6	1981.35	1980.92	20°	19.714°	222.276°	215.124°	0.0	.000233
7	1822.20	1821.78	179.5°	179.518°	222.276°	227.503°	0.0	.000225
8	1981.35	1981.09	179.5°	179.523°	222.276°	225.400°	0.0	.000138
9	1822.20	1821.78	170°	169.801°	222.276°	230.347°	0.0	.000225
10	1981.35	1981.08	170°	169.859°	222.276°	229.337°	0.0	.000144
11	1822.20	1821.81	160°	159.581°	222.276°	230.052°	0.0	.000229
12	1981.35	1981.06	160°	159.690°	222.276°	229.113°	0.0	.000165

Table 1. Initial and Final Values of the Orbit Elements.

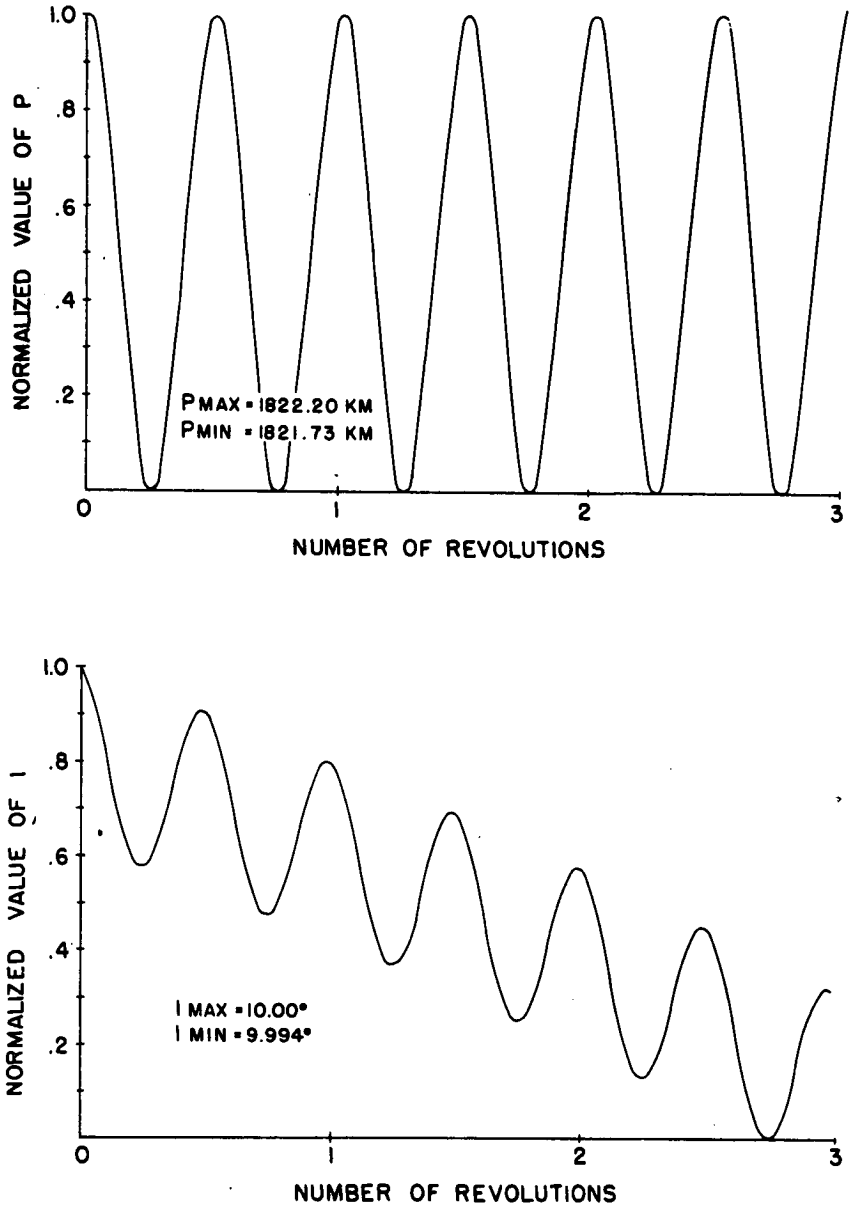

SEMI-LATUS RECTUM AND INCLINATION VS.
NUMBER OF REVOLUTIONS FOR ORBIT TYPE 3

FIGURE 5

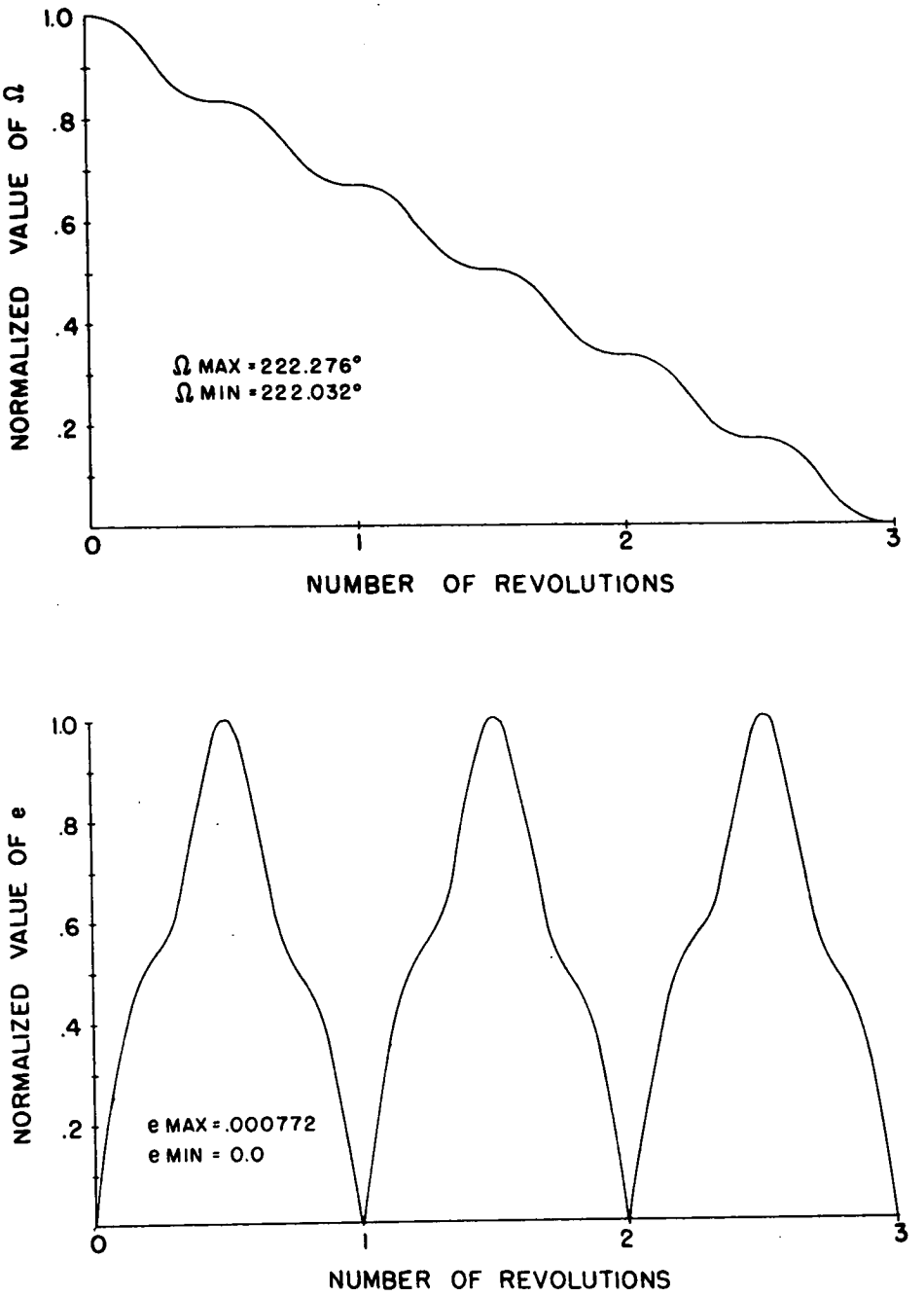

LONGITUDE OF ASCENDING NODE AND ECCENTRICITY VS. NUMBER OF REVOLUTIONS FOR ORBIT TYPE 3

FIGURE 6

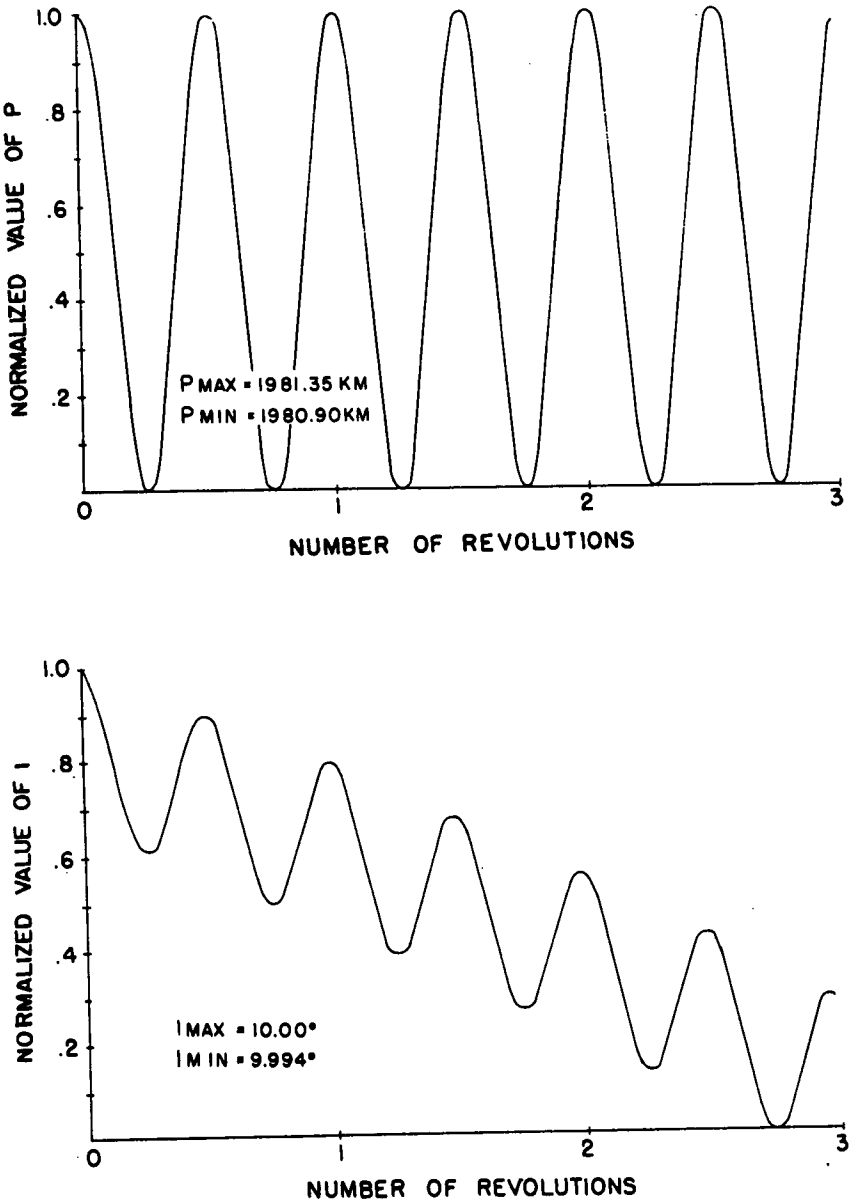

SEMI-LATUS RECTUM AND INCLINATION VS.
NUMBER OF REVOLUTIONS FOR ORBIT TYPE 4

FIGURE 7

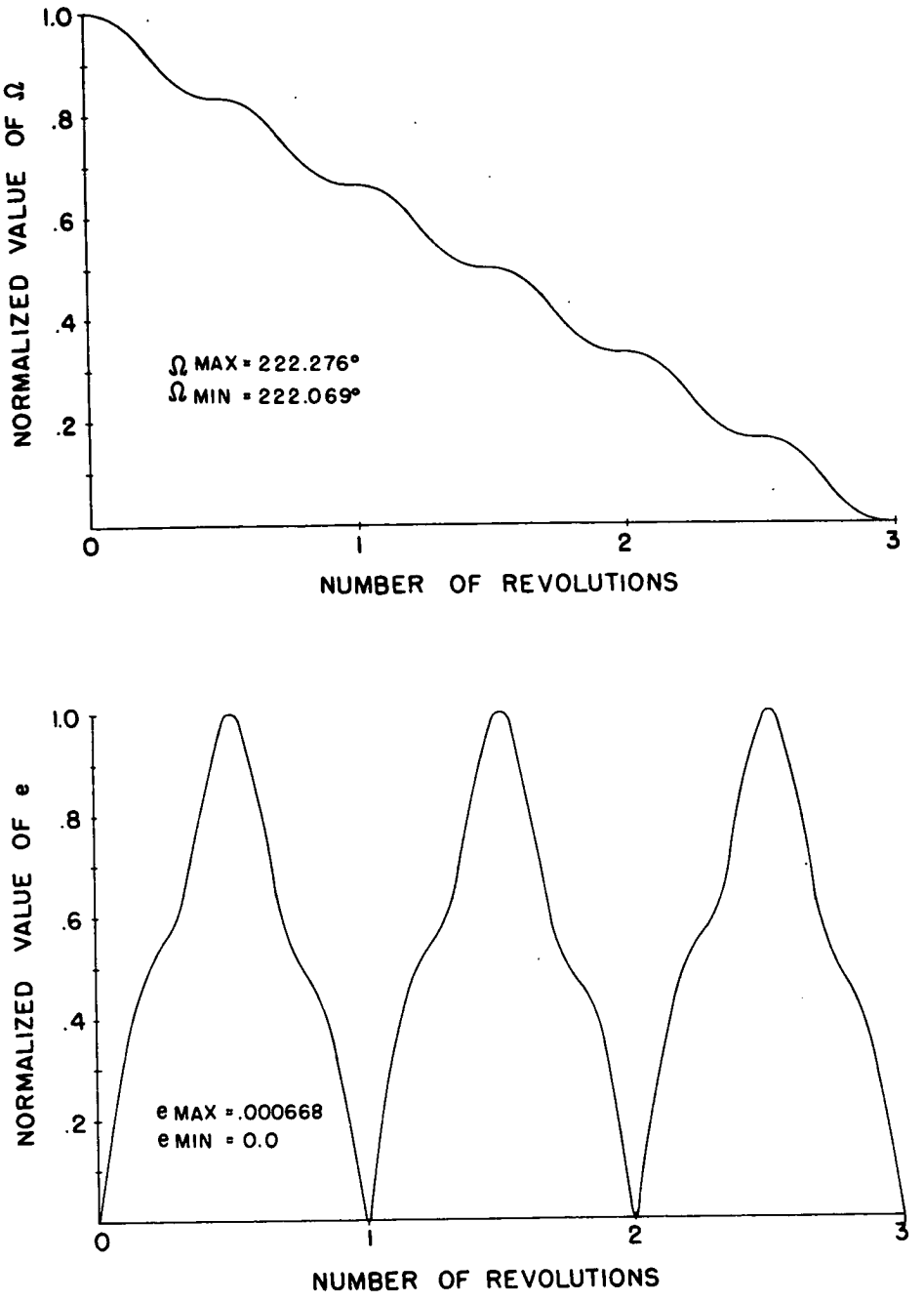

LONGITUDE OF ASCENDING NODE AND ECCENTRICITY VS. NUMBER OF REVOLUTIONS FOR ORBIT TYPE 4

FIGURE 8

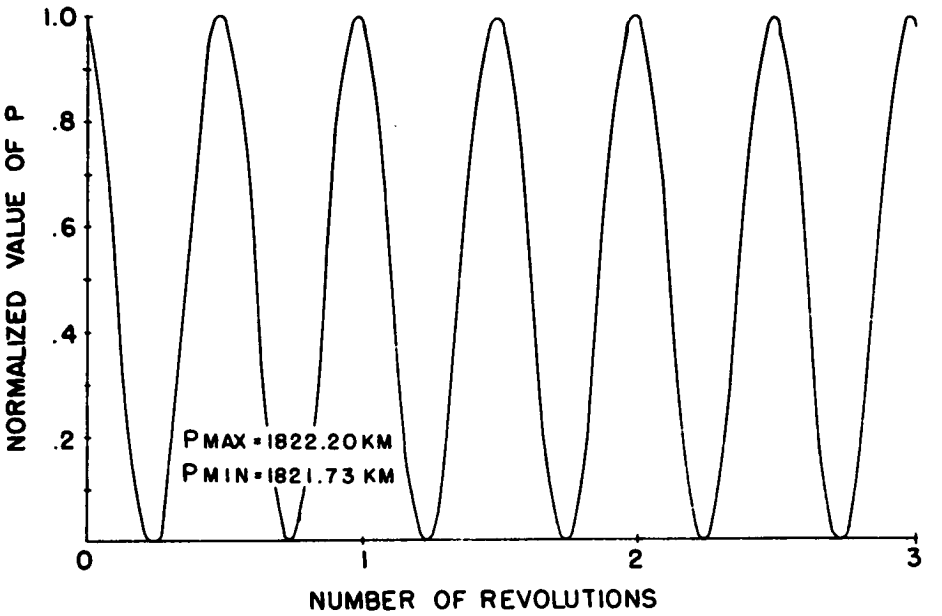

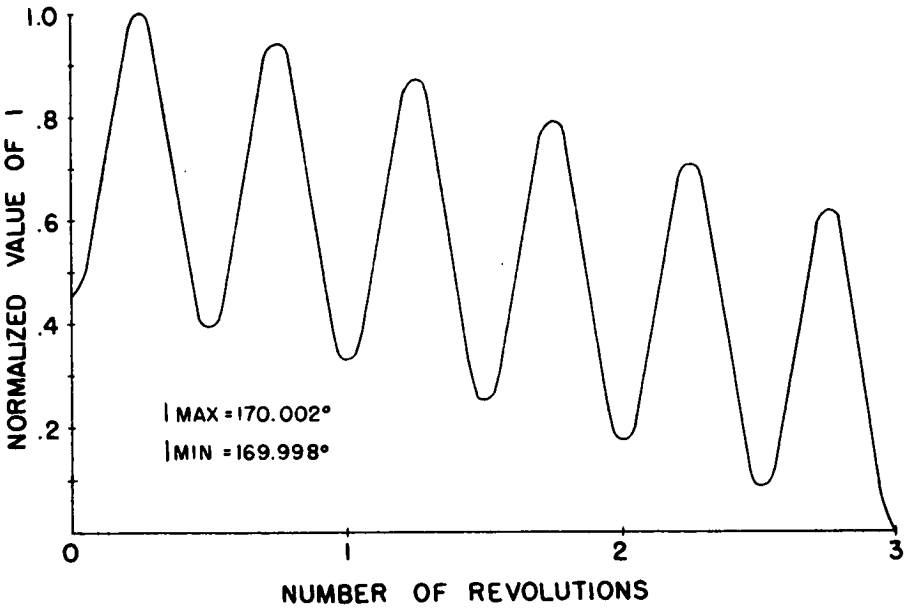

SEMI-LATUS RECTUM AND INCLINATION VS.
NUMBER OF REVOLUTIONS FOR ORBIT TYPE 9

FIGURE 9

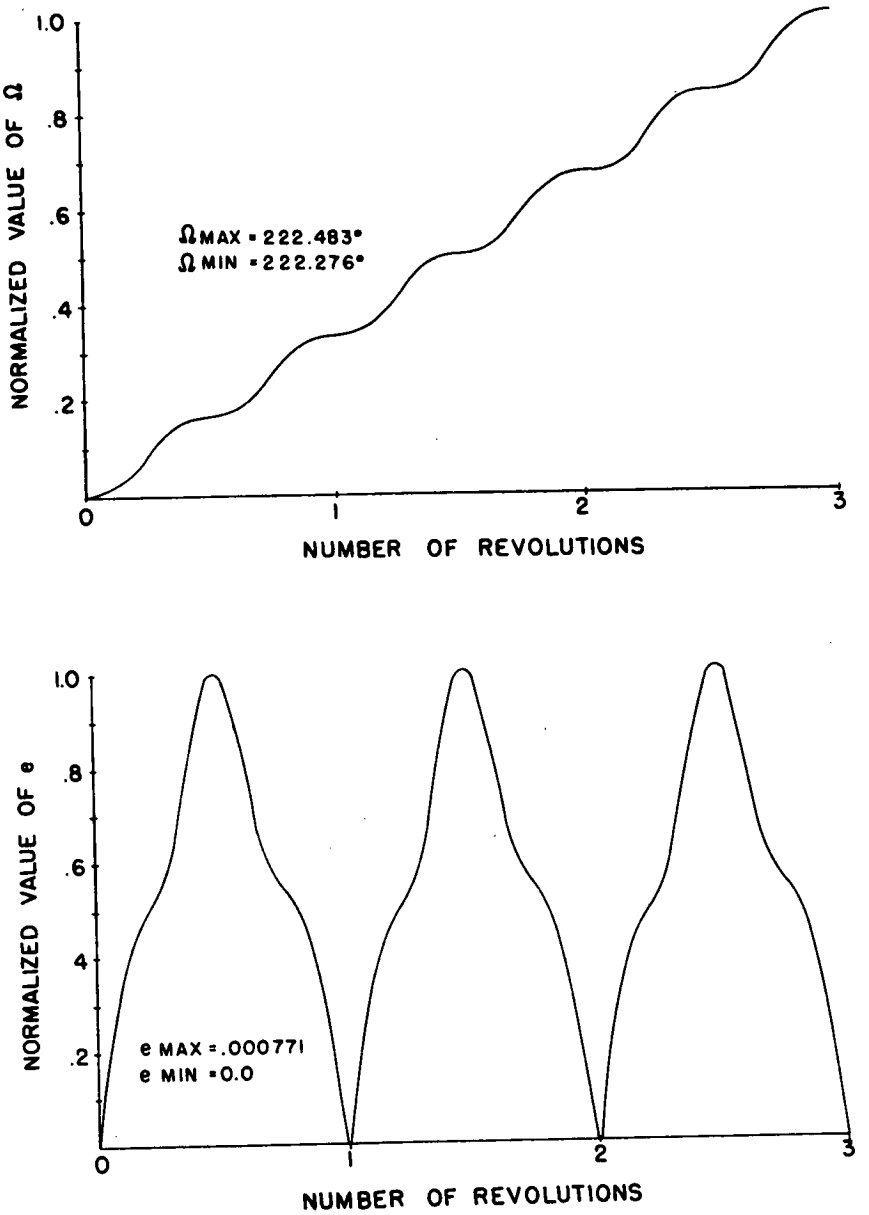

LONGITUDE OF ASCENDING NODE AND ECCENTRICITY VS. NUMBER OF REVOLUTIONS FOR ORBIT TYPE 9

FIGURE 10

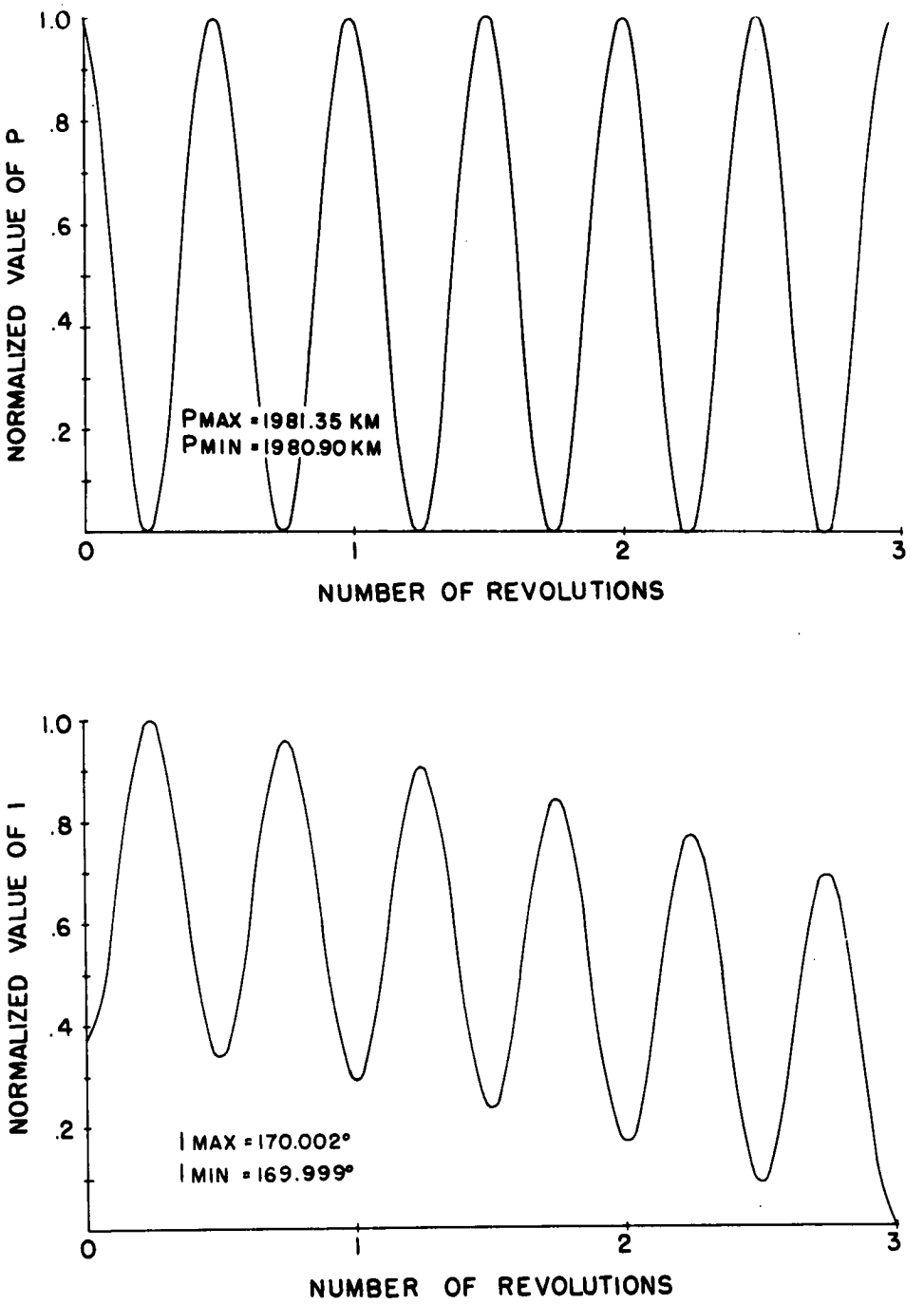

SEMI-LATUS RECTUM AND INCLINATION VS.
NUMBER OF REVOLUTIONS FOR ORBIT TYPE 10

FIGURE 11

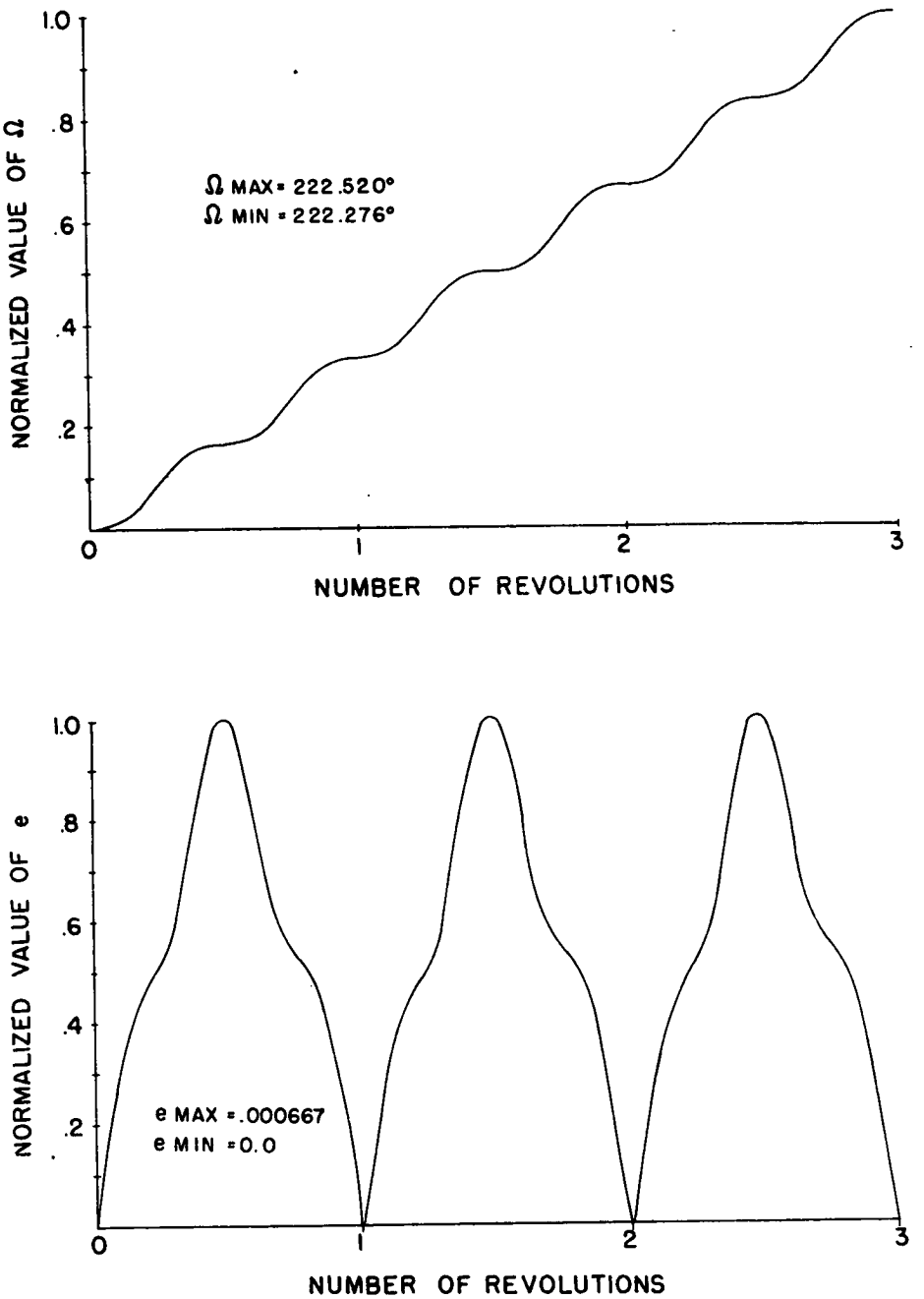

LONGITUDE OF ASCENDING NODE AND ECCENTRICITY VS. NUMBER OF REVOLUTIONS FOR ORBIT TYPE 10

FIGURE 12

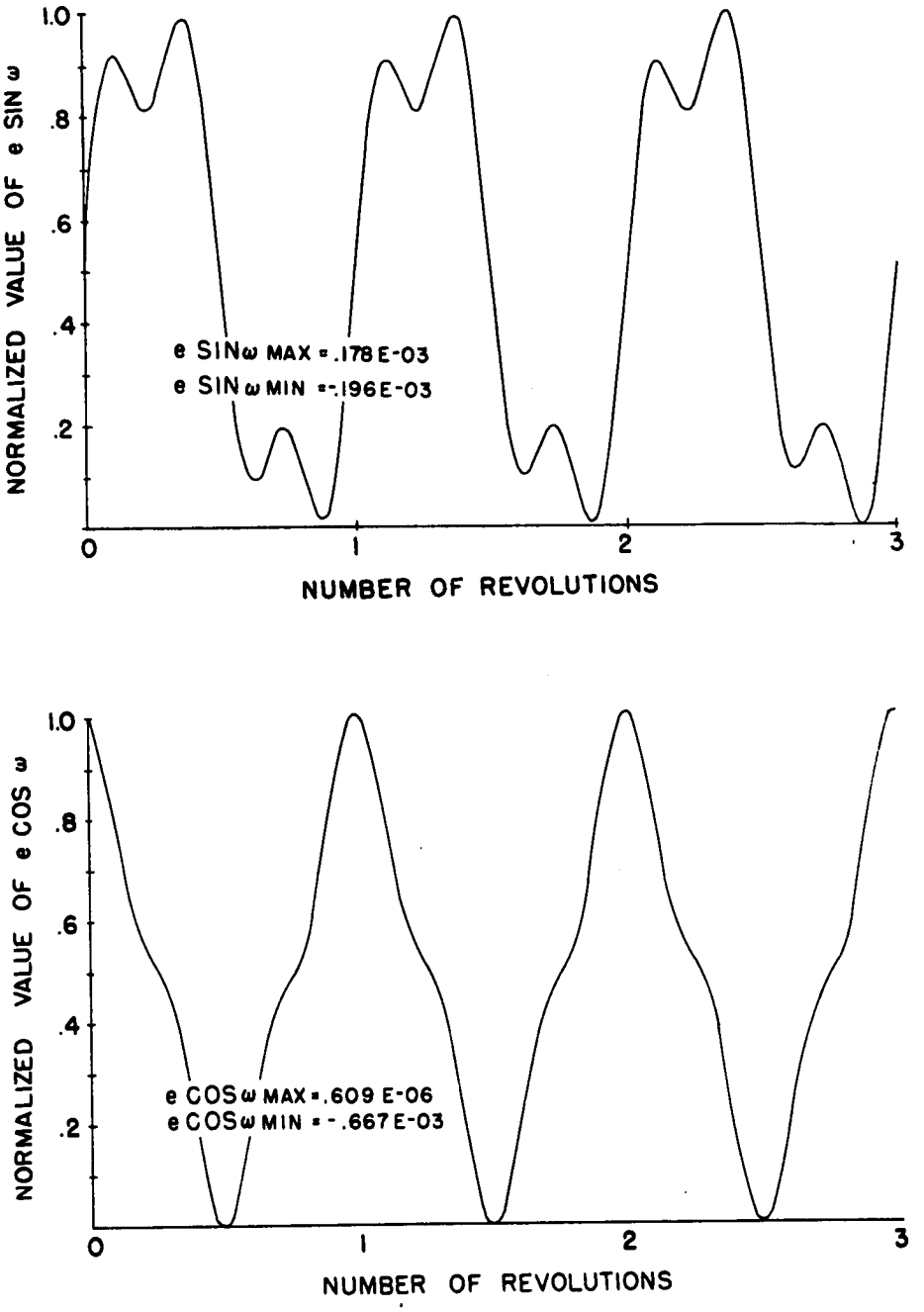

ECCENTRICITY X SINE (ARGUMENT OF PERISELENE) AND ECCENTRICITY X COSINE (ARGUMENT OF PERISELENE) VS. NUMBER OF REVOLUTIONS FOR ORBIT TYPE 10

FIGURE 13

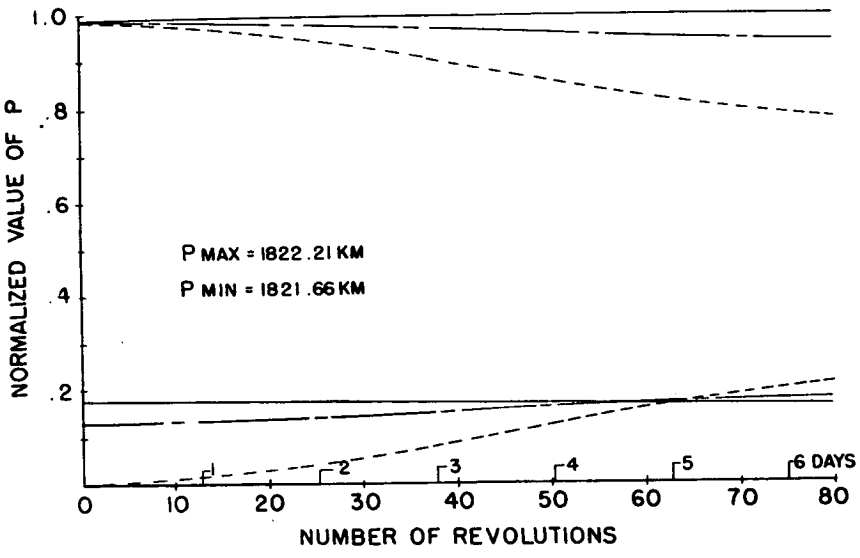

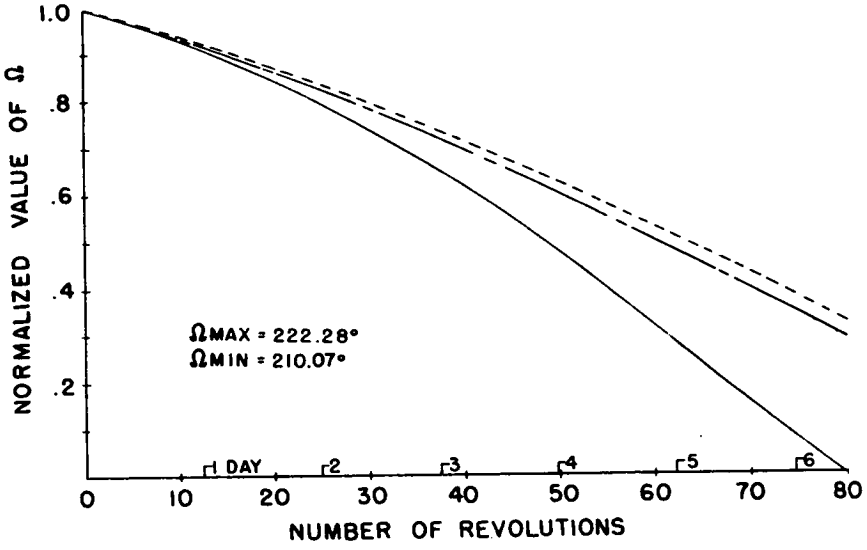

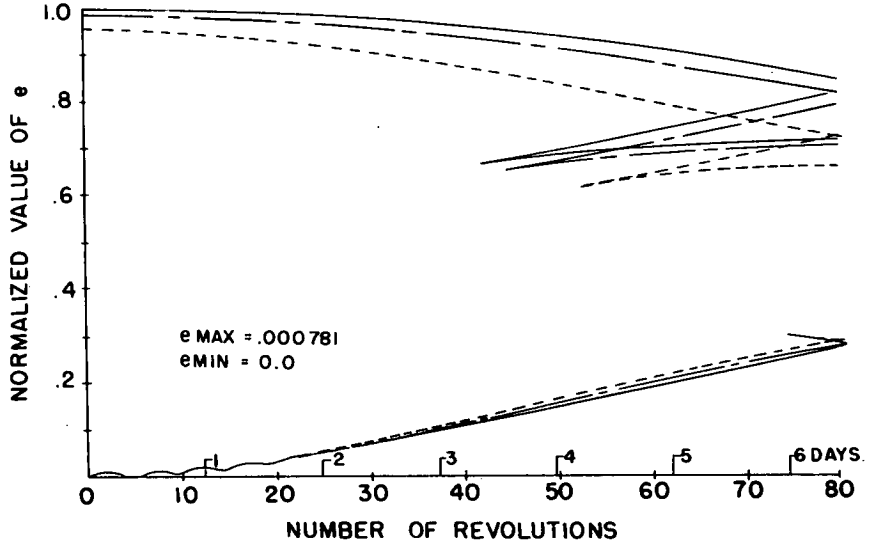

SEMI-LATUS RECTUM, LONGITUDE OF ASCENDING NODE AND ECCENTRICITY VS. NUMBER OF REVOLUTIONS FOR ORBIT TYPES 1,3,5

——— ORBIT TYPE 1, I = .50°

— — — ORBIT TYPE 3, I = 10°

------- ORBIT TYPE 5, I = 20°

FIGURE 14

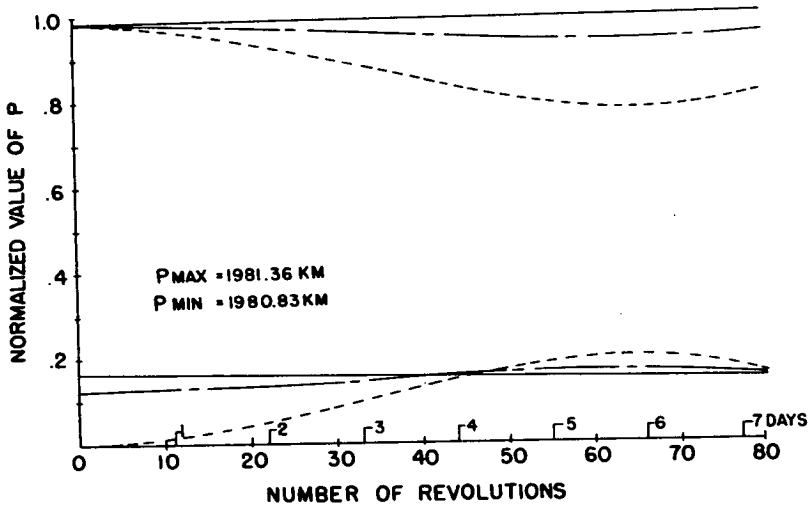

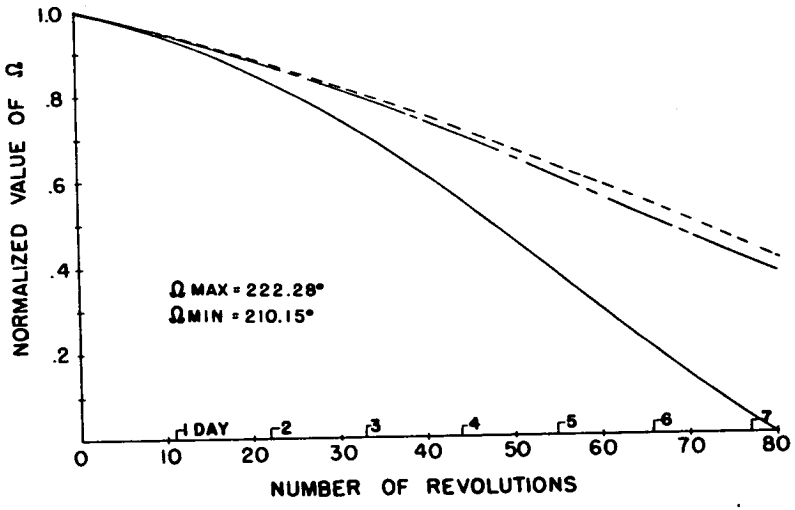

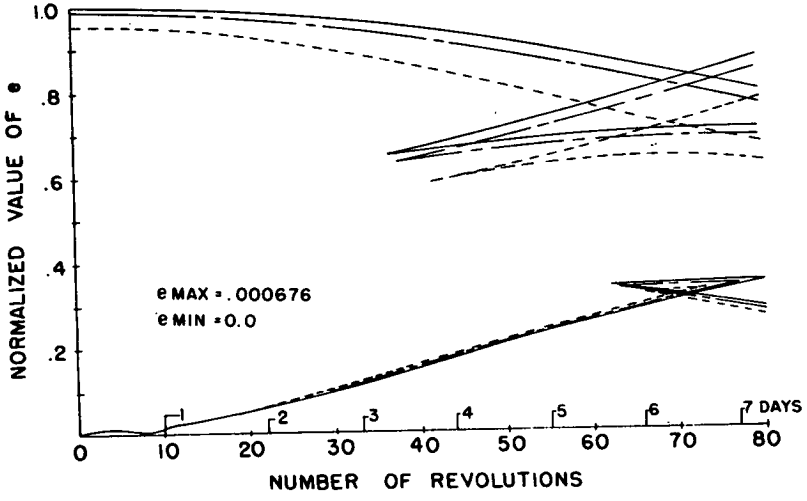

SEMI-LATUS RECTUM, LONGITUDE OF ASCENDING NODE AND ECCENTRICITY VS. NUMBER OF REVOLUTIONS FOR ORBIT TYPES 2, 4, 6

——— ORBIT TYPE 2, I = .50°
—— — ORBIT TYPE 4, I = 10°
------- ORBIT TYPE 6, I = 20°

FIGURE 15

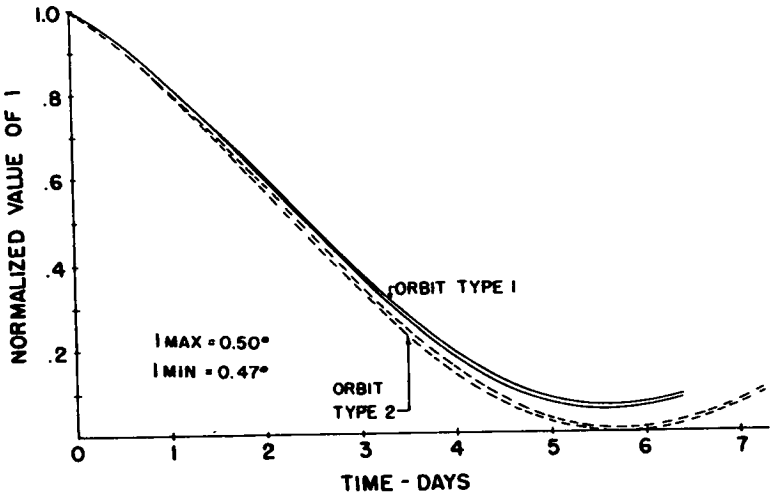

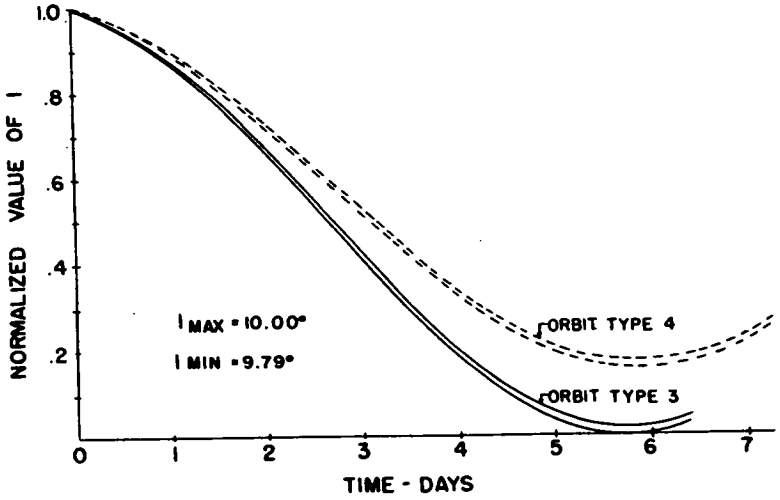

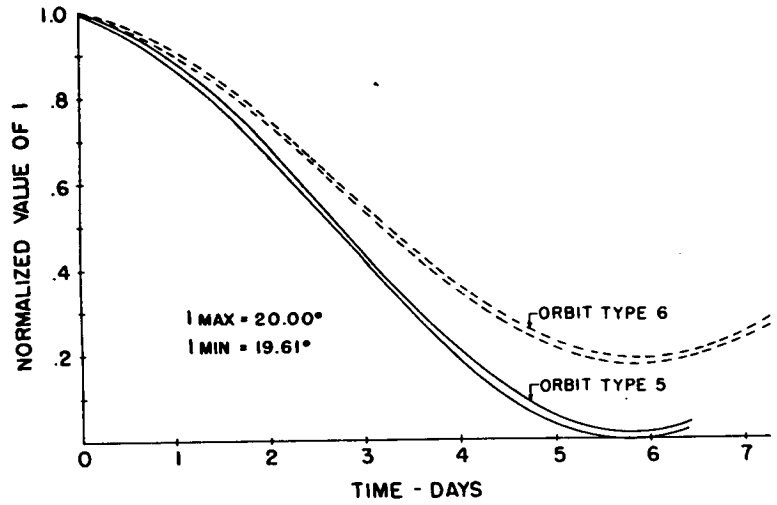

INCLINATION VS. TIME FOR ORBIT TYPES I THROUGH 6

——— P = 1822.20 KM

------ P = 1981.35 KM

FIGURE 16

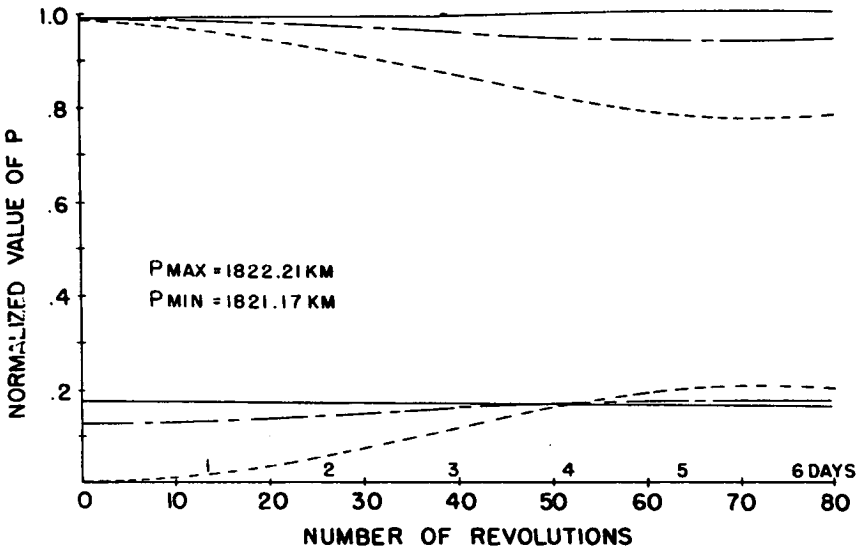

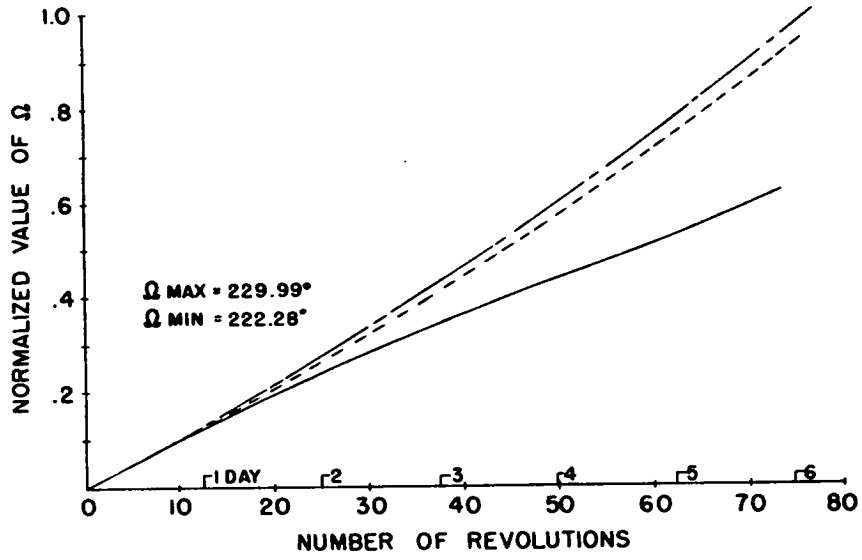

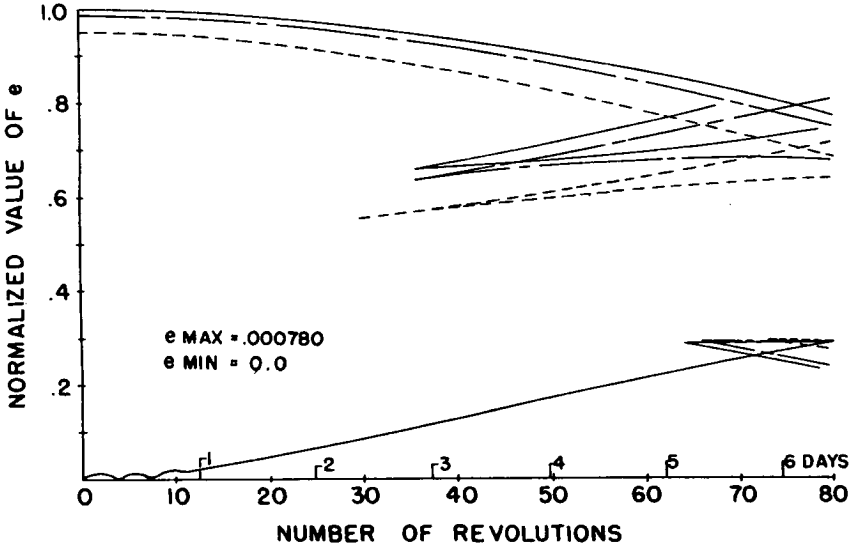

SEMI-LATUS RECTUM, LONGITUDE OF ASCENDING NODE AND ECCENTRICITY VS. NUMBER OF REVOLUTIONS FOR ORBIT TYPES, 7, 9, 11

——— ORBIT TYPE 7, i=179.5°

— — — ORBIT TYPE 9, i=170°

------ ORBIT TYPE 11, i=160°

FIGURE 17

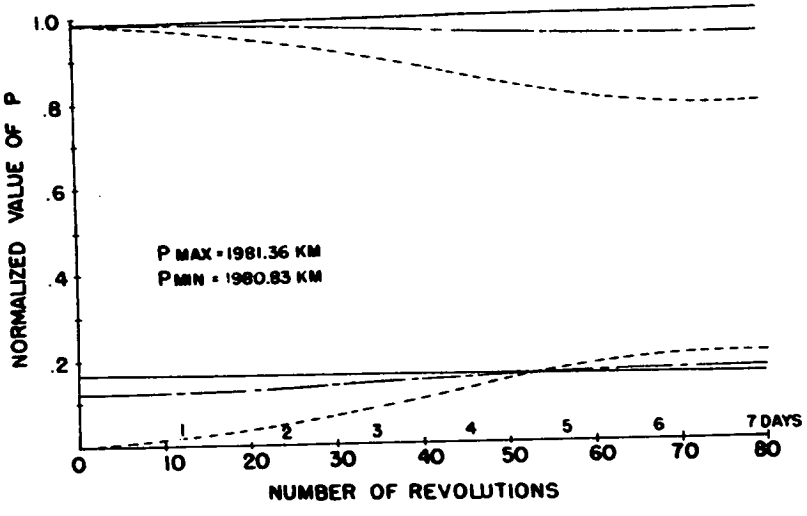

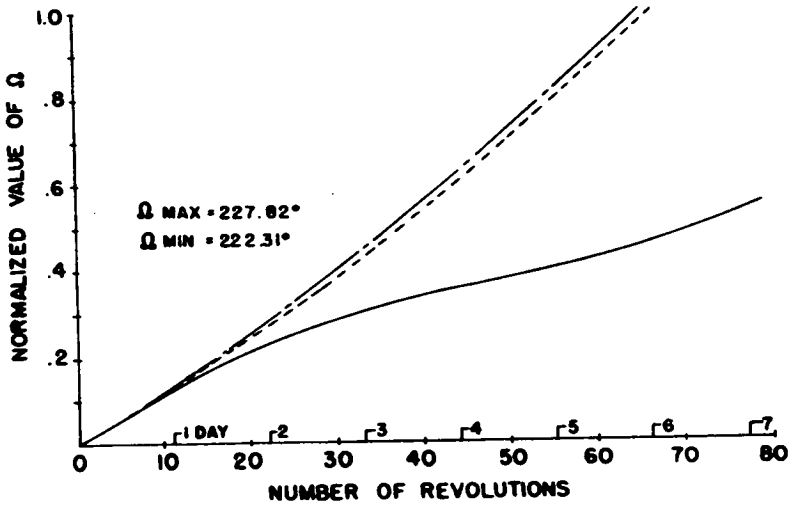

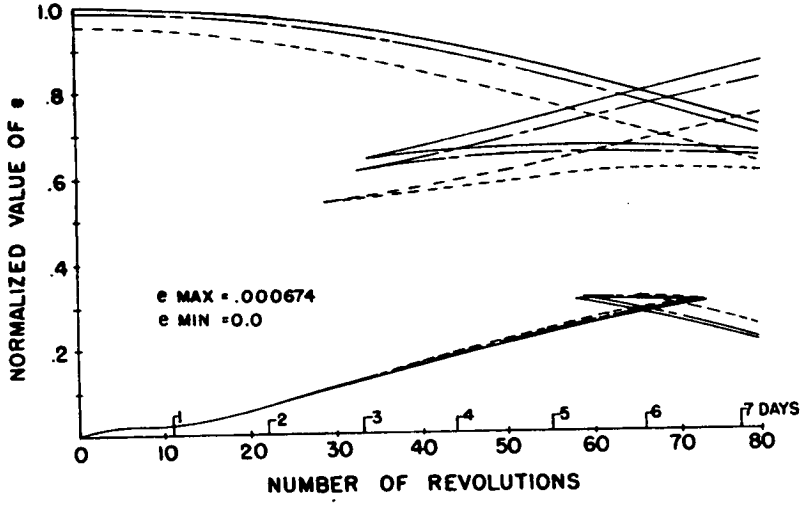

SEMI-LATUS RECTUM, LONGITUDE OF ASCENDING NODE AND ECCENTRICITY VS. NUMBER OF REVOLUTIONS FOR ORBIT TYPES 8,10,12

——— ORBIT TYPE 8, I = 179.5°

—·—·— ORBIT TYPE 10, I = 170°

------ ORBIT TYPE 12, I = 160°

FIGURE 18

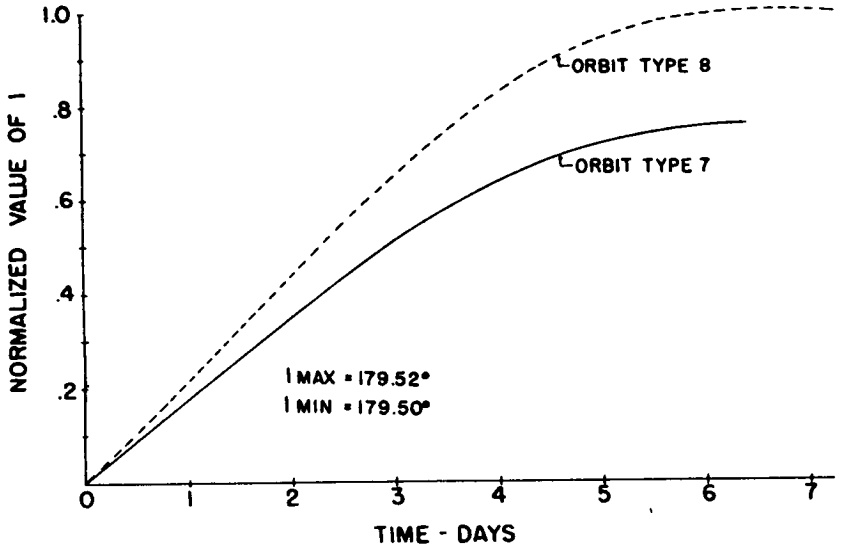

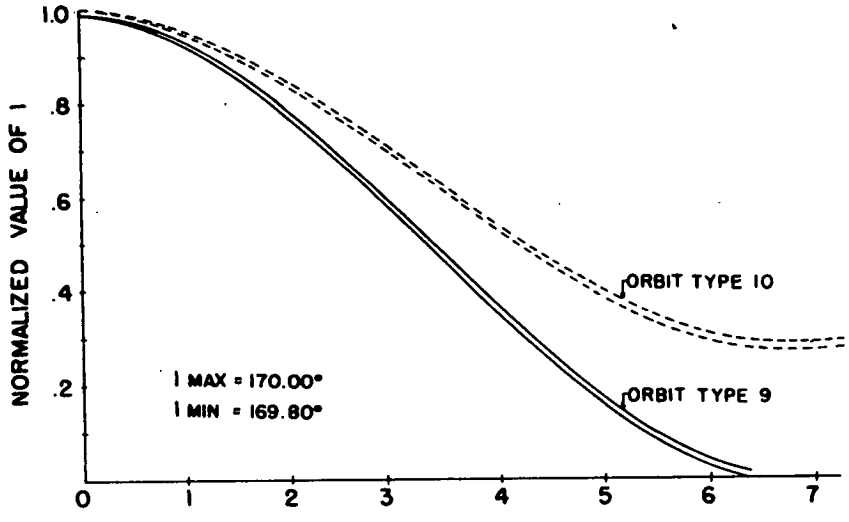

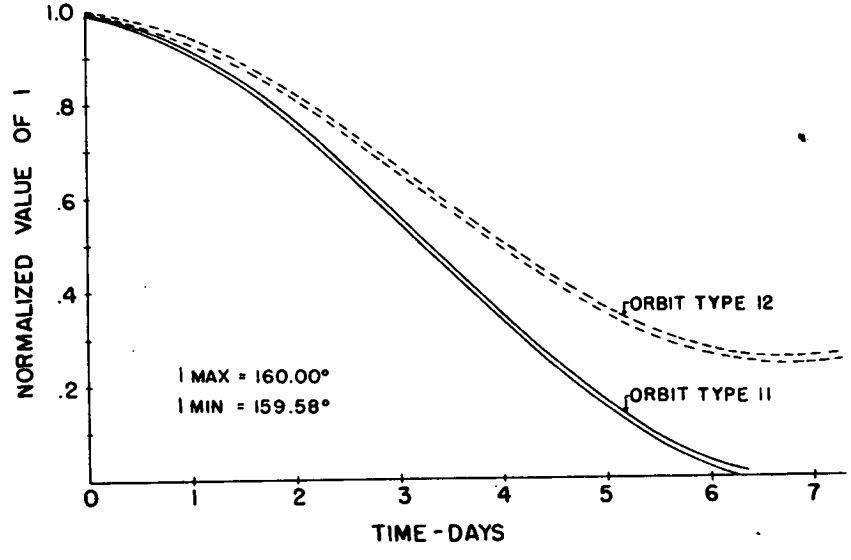

INCLINATION VS. TIME FOR ORBIT TYPES 7 THROUGH 12

——— P = 1822.20 KM

- - - - - - P = 1981.35 KM

FIGURE 19

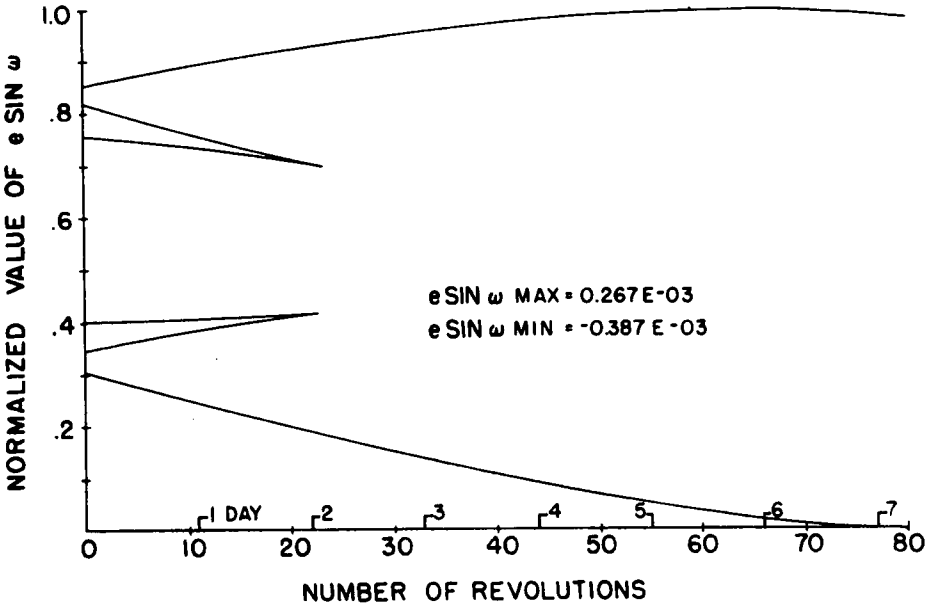

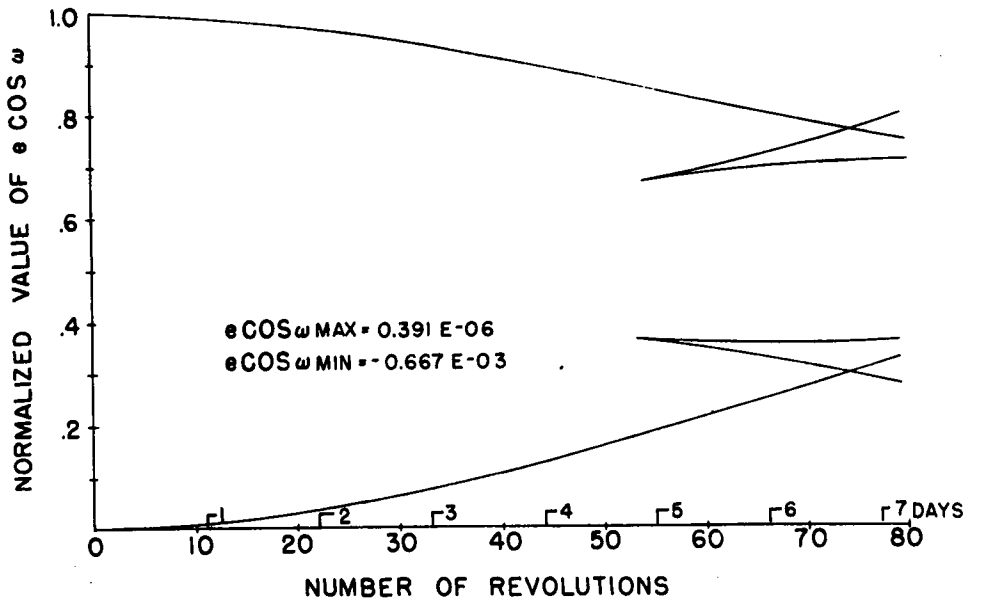

ECCENTRICITY X SINE (ARGUMENT OF PERISELENE) AND ECCENTRICITY X COSINE (ARGUMENT OF PERISELENE) VS. NUMBER OF REVOLUTIONS FOR ORBIT TYPE 10

FIGURE 20

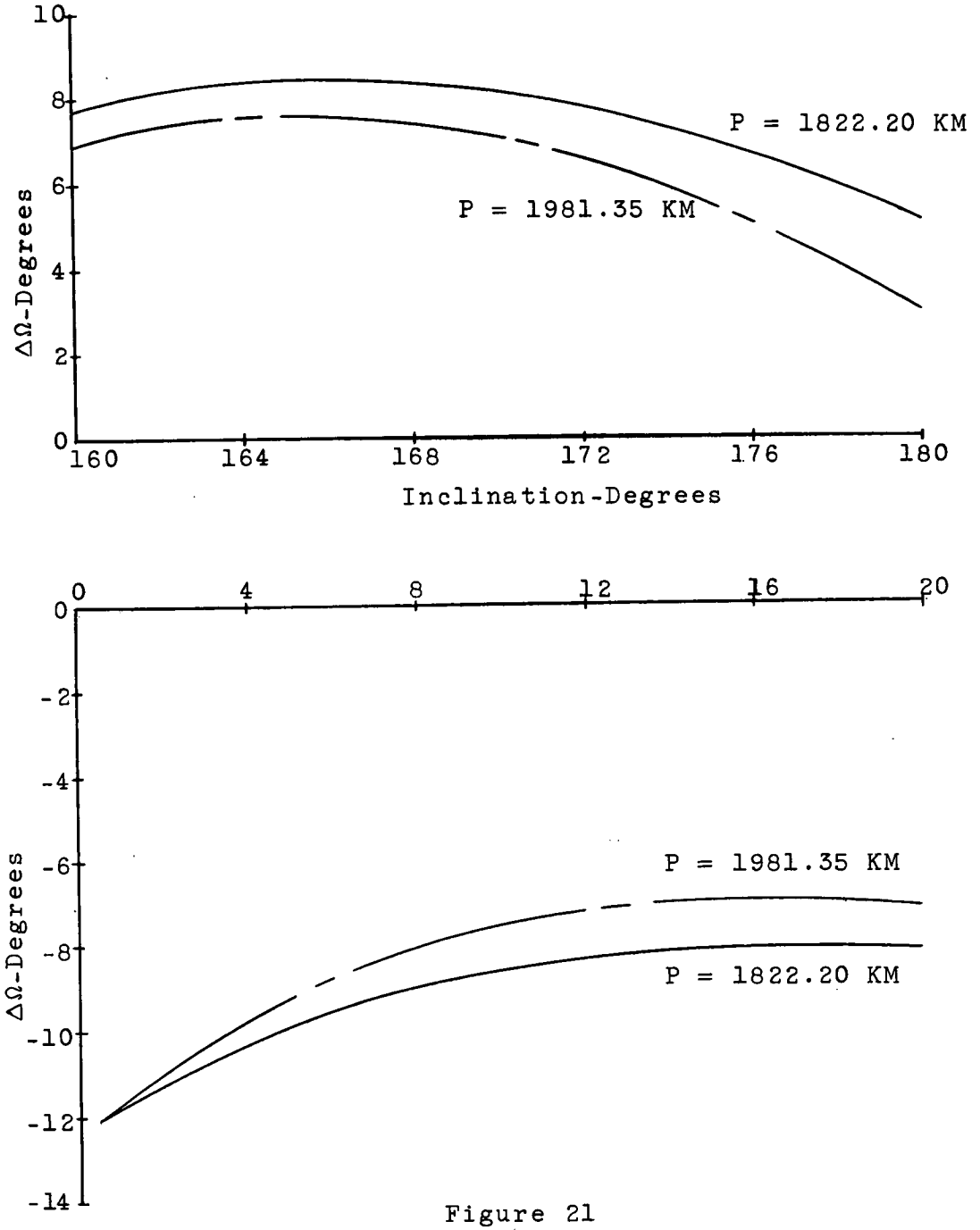

Figure 21

Change in Longitude of Ascending Node after 80 Revolutions vs. Inclination

V. CONCLUSION AND RECOMMENDATIONS

A numerical integration scheme was revised to integrate a set of differential equations which describe the time rates of change of the satellite orbit elements but which does not have the small eccentricity restriction of Lagrange's Planetary Equations. This scheme was used to predict the variation of the orbit elements of Apollo-type lunar orbits over a period of 80 satellite revolutions. Computation was carried out on the CDC 1604 digital computer.

The following conclusions are drawn from the results obtained from this study.

1. All orbit types considered exhibit a high degree of stability for a period of 80 revolutions, and there is no indication of future instability. However, it should be noted that the time periods considered here are not suitable for answering questions about the long-term behavior of the satellite.

2. The inclination of the radius vector of the Earth to the lunar equator is such that the component of the

Earth's perturbing force normal to the plane of the satellite's orbit on orbit types 1 through 6 (prograde) and 7 and 8 (retrograde) is in the opposite direction from that on orbit types 9 through 12 (retrograde) throughout the time period considered here. Consequently, the effect of the Earth is to cause a regression of the node for orbit types 1 through 8 and a progression for orbit types 9 through 12.

3. The line of nodes progresses for retrograde orbits and regresses for prograde orbits. The rate of change of Ω decreases with altitude for a given inclination. It also decreases with increasing inclination for a given altitude.

4. Eccentricity and semi-latus rectum appear to oscillate with a relatively constant amplitude for all of the orbit types considered here.

5. A fairly complete picture of the variation of the orbit elements for an Apollo-type lunar orbit may be obtained from a study of the results presented here.

Considerable additional work needs to be done in this area to determine more completely the characteristics of lunar satellite orbits. The areas of interest are:

1. Since satellites for future lunar exploration will undoubtedly be placed in orbits of widely varying altitude, inclination and eccentricity, the effects of varying these parameters over a wider range than was considered here should be determined.

2. Integration of the perturbation equations over a longer time period, preferably an entire month, to more fully ascertain the effects of the Earth would be worthwhile.

3. The expansion of the computer program used here to include the effects of the Sun would give a positive indication of their relative importance.

4. Since the amount of computer time required to integrate the perturbation equations for a given number of revolutions becomes prohibitive for orbits of high altitude, it is important that more sophisticated analytical solutions to the perturbation equations be developed. Results for existing closed form solutions should be compared with numerical solutions to determine their degree of accuracy and where needed more exact methods should be determined.

R E F E R E N C E S

1. Battin, R. H. Astronautical Guidance, McGraw-Hill Book Co., New York, 1964.

2. Brouwer, D., and G. M. Clemence, Methods of Celestial Mechanics, Academic Press, New York, 1961.

3. Brumberg, V. A.; S. N. Kirpichnikov; G. A. Chebrotarev; "Orbits of Artificial Moon Satellites," Soviet Astronomy, July-August, 1961, pp. 95-105.

4. Clarke, V. C., Jr. "Constants and Related Data Used in Trajectory Calculations at the Jet Propulsion Laboratories," Technical Report No. 32-273, May 1, 1962.

5. Goddard, D. S. "The Motion of a Near Lunar Satellite," M.S. Thesis, The University of Texas, August, 1963.

6. Hildebrand, F. B. Introduction to Numerical Analysis, McGraw-Hill Book Co., Inc., New York, 1956.

7. Kalensher, B. E. "Selenographic Coordinates," JPL Technical Report No. 32-41, February, 1961.

8. Memoirs of the Royal Astronomical Society, Vol. LVII, pp. 109-145.

9. Memorandum to Distribution from Director, Aeroballistics Division, MSFC, Subject: Conference on Astronomical and Geodetic Constants (Earth and Lunar Models) held at GSFC on May 16, 1963, dated May 20, 1963.

10. Lass, H., and C. Solloway, "Motion of a Satellite of the Moon," ARS Jr., February, 1961, pp. 220-221.

11. Lorell, J. "Characteristics of Lunar Satellite Orbits," Jet Propulsion Laboratories, Technical Memorandum 312-164, February, 1962.

12. McCuskey, S. W. Introduction to Celestial Mechanics, Addison-Wesley Publishing Co., Inc., Reading, Mass., 1963.

13. Plummer, H. C. An Introductory Treatise on Dynamical Astronomy, Dover Publications, Inc., New York, 1960.

14. Small, H. W. "The Motion of a Satellite about an Oblate Earth," Lockheed Missiles and Space Co., Report No. LMSC/A086756, November, 1961.

15. Tolson, R. H. "The Motion of a Lunar Satellite Under the Influence of the Moon's Noncentral Force Field," M.S. Thesis, Virginia Polytechnic Inst., April, 1963.